



**HAL**  
open science

## Potential for virus endogenization in humans through testicular germ cell infection: the case of HIV

Dominique Mahé, Giulia Matusali, Claire Deleage, R Alvarenga, Anne-Pascale Satie, A Pagliuzza, Romain Mathieu, Sylvain Lavoué, Bernard Jégou, Luiz R de França, et al.

### ► To cite this version:

Dominique Mahé, Giulia Matusali, Claire Deleage, R Alvarenga, Anne-Pascale Satie, et al.. Potential for virus endogenization in humans through testicular germ cell infection: the case of HIV. *Journal of Virology*, 2020, 94 (24), 10.1128/JVI.01145-20 . hal-02964526

**HAL Id: hal-02964526**

**<https://hal.science/hal-02964526>**

Submitted on 12 Oct 2020

**HAL** is a multi-disciplinary open access archive for the deposit and dissemination of scientific research documents, whether they are published or not. The documents may come from teaching and research institutions in France or abroad, or from public or private research centers.

L'archive ouverte pluridisciplinaire **HAL**, est destinée au dépôt et à la diffusion de documents scientifiques de niveau recherche, publiés ou non, émanant des établissements d'enseignement et de recherche français ou étrangers, des laboratoires publics ou privés.



Distributed under a Creative Commons Attribution 4.0 International License

1 **Potential for virus endogenization in humans through testicular germ cell infection: the**  
2 **case of HIV**

3

4 Dominique Mahé<sup>1</sup>, Giulia Matusali<sup>1</sup>, Claire Deleage<sup>1\*</sup>, Raquel L. L. S. Alvarenga<sup>2</sup>, Anne-  
5 Pascale Satie<sup>1</sup>, Amélie Pagliuzza<sup>3</sup>, Romain Mathieu<sup>4</sup>, Sylvain Lavoué<sup>5</sup>, Bernard Jégou<sup>1</sup>, Luiz  
6 R. de França<sup>2</sup>, Nicolas Chomont<sup>3</sup>, Laurent Houzet<sup>1</sup>, Antoine D. Rolland<sup>1</sup>, Nathalie Dejudcq-  
7 Rainsford<sup>1#</sup>

8

9 <sup>1</sup> Univ Rennes, Inserm, EHESP, Irset (Institut de recherche en santé, environnement et travail)  
10 - UMR\_S1085, F-35000 Rennes, France

11 <sup>2</sup> Laboratory of Cellular Biology, Department of Morphology, Federal University of Minas  
12 Gerais, Belo Horizonte, Brazil

13 <sup>3</sup> Department of Microbiology, Infectiology and Immunology, Faculty of Medecine,  
14 Université de Montréal, and Centre de recherche du CHUM, Montréal, Quebec, Canada

15 <sup>4</sup> Centre Hospitalier Universitaire de Pontchaillou, Service Urologie, Rennes, France

16 <sup>5</sup> Centre Hospitalier Universitaire de Pontchaillou, Centre de Coordination des prélèvements,  
17 Rennes, France

18

19

20 #Corresponding author: Nathalie DEJUCQ-RAINSFORD, IRSET-Inserm U1085, 9 avenue  
21 du Pr Léon Bernard, F-35000 Rennes, France. E-mail : [nathalie.dejudcq-rainsford@inserm.fr](mailto:nathalie.dejudcq-rainsford@inserm.fr).  
22 Phone : +33 2 2323 5069

23

24

25 \*Present address: Claire Deleage, AIDS and Cancer Virus Program, Leidos Biomedical  
26 Research, Inc. Frederick National Laboratory for Cancer Research, Frederick, Maryland,  
27 USA.

28

29

30 **Short title:** HIV infection of the germ line

31 **Key words:** virus, HIV, SIV, testis, germ line, spermatogenesis, gametes, entry, integration,  
32 replication, endogenization

33 **Abstract**

34

35 Viruses have colonized the germ line of our ancestors at several occasions during evolution,  
36 leading to the integration in the human genome of viral sequences from over 30 retroviral  
37 groups and a few non-retroviruses. Among the recently emerged viruses infecting humans,  
38 several target the testis (eg HIV, Zika and Ebola viruses). Here we aimed to investigate  
39 whether human testicular germ cells (TGCs) can support integration by HIV, a contemporary  
40 retrovirus that started to spread in the human population during the last century. We report  
41 that albeit alternative receptors enabled HIV-1 binding to TGCs, HIV virions failed to infect  
42 TGCs *in vitro*. Nevertheless, exposure of TGCs to infected lymphocytes, naturally present in  
43 the testis from HIV+ men, led to HIV-1 entry, integration and early protein expression.  
44 Similarly, cell-associated infection or bypassing viral entry led to HIV-1 integration in a  
45 spermatogonial cell line. Using DNAscope, HIV-1 and SIV DNA were detected within a few  
46 TGCs in the testis from one infected patient, one rhesus macaque and one African Green  
47 monkey *in vivo*. Molecular landscape analysis revealed that early TGCs were enriched in HIV  
48 early co-factors up to integration and had overall low antiviral defenses when compared with  
49 testicular macrophages and Sertoli cells. In conclusion, our study reveals that TGCs can  
50 support the entry and integration of HIV upon cell-associated infection. This could represent a  
51 way for this contemporary virus to integrate our germline and become endogenous in the  
52 future, as happened during human evolution for a number of viruses.

53

54 **Importance**

55 Viruses have colonized the host germ line at many occasions during evolution to eventually  
56 become endogenous. Here we aimed at investigating whether human testicular germ cells

57 (TGCs) can support such viral invasion by studying HIV interactions with TGCs *in vitro*. Our  
58 results indicate that isolated primary TGCs express alternative HIV-1 receptors allowing  
59 virions binding but not entry. However, HIV-1 entered and integrated in TGCs upon cell-  
60 associated infection, and produced low level of viral proteins. *In vivo*, HIV-1 and SIV DNA  
61 was detected in a few TGCs. Molecular landscape analysis showed that TGCs have overall  
62 weak antiviral defenses. Altogether, our results indicate that human TGCs can support HIV-1  
63 early replication including integration, suggesting potential for endogenization in the future  
64 generations.

65

66 **Introduction**

67 Retroviruses have repeatedly infected the germline during our evolution and integrated their  
68 DNA into the host genome , which has been passed on to the next generations by Mendelian  
69 inheritance (1, 2). When not detrimental, the integration of viral sequences has led to their  
70 fixation and endogenization in the population (3). Thus, about 8% of the human genome is  
71 now composed of endogenous retroviruses (ERVs), representing 31 distinct viral groups (2).  
72 Such integration, still ongoing in mammals (4), has driven the acquisition of new functions in  
73 the host, including a protective role against exogenous infections (5, 6). Within the retrovirus  
74 family, several lentiviruses have been endogenized in mammals, including SIV in pro-  
75 lemurians (7–12). A few non-retroviruses have also colonized the germline of their host but  
76 the mechanisms for their integration are unclear (1).

77 HIV-1 is an emerging zoonotic lentivirus that has infected over 70 million people since its  
78 worldwide spreading in the human population from the beginning of the 1980s. Current  
79 antiretroviral treatments effectively control but do not eradicate the virus, which still  
80 represents a major threat for the human population, with an average of nearly 2 million new  
81 infections each year. Horizontal transmission through semen plays a key role for HIV-1  
82 dissemination, and is most likely mediated by the free viral particles and infected leukocytes  
83 present in this fluid (13). We and others found that HIV/SIV strains in semen are locally  
84 produced in a subset of individuals (reviewed in (13)) and arise from several organs within the  
85 male genital tract (14). Interestingly, HIV-1 can associate with spermatozoa *in vitro* (15) and  
86 was detected by some authors in a small proportion of patients' sperm (16–25). Since  
87 spermatozoa have a highly compact nucleus and are transcriptionally silent, this detection  
88 may suggest infection of their germ cell progenitors in the testis.

89 The testis is an immune-privilege organ with restricted drugs penetration, considered to  
90 constitute a tissue reservoir for HIV and other emerging viruses such as Zika and Ebola (1,  
91 26, 27). HIV-1 productively infects testicular T lymphocytes and resident macrophages,  
92 which are naturally localized in close proximity to the early germ cells present in the basal  
93 compartment of the seminiferous epithelium and therefore outside the blood testis/Sertoli cell  
94 barrier (27–31). A couple of early studies reported HIV nucleic acids in isolated cells  
95 resembling germ cells within the seminiferous tubules of deceased patients using *in situ* PCR,  
96 a controverted technique suspected of generating false positives (30, 32, 33). These findings  
97 have therefore been largely dismissed (34, 35). Furthermore, the detection of viral RNA in  
98 TGCs could reflect an accumulation of virions bound to the cell surface rather than a true  
99 infection. Unfortunately, the scarce access to testicles of HIV-1+ men has hindered further  
100 investigations on this debated issue (35). SIV RNA and proteins were later described in TGCs  
101 from non-human primates, using *in situ* hybridization and immunohistochemistry (36, 37).  
102 Whether human TGCs are infected by HIV and to which extent remains an open question.

103 In this study, we aimed to investigate whether human TGCs support HIV entry and  
104 integration as a proxy to evaluate potential for viral colonization in the next generations'  
105 human genome. We found that HIV-1 binds to primary TGCs, but that viral entry was  
106 inefficient. However, virus integration and early viral protein expression were observed  
107 following cell-associated infection. *In vivo*, testicular germ cells harboring viral DNA were  
108 detected in the testis from an HIV-infected individual using next generation *in situ*  
109 hybridization DNAscope. SIV-infected TGCs were also detected in one experimentally-  
110 infected rhesus macaque and one African Green monkey, a natural host for SIV. To determine  
111 whether human TGC had evolved elevated defense mechanisms to prevent vertical  
112 transmission of viral sequences to the offspring and thus potential endogenization, we  
113 analyzed the molecular landscape of TGCs and compared it with that of HIV-permissive and

114 non-permissive testicular somatic cells using single-cell RNA-sequencing data. This analysis  
115 revealed relatively low gene expression levels for viral sensors and HIV early life cycle  
116 inhibitors in TGCs, together with an enrichment in HIV early co-factors in spermatogonia.  
117 Overall, our study provides the proof of concept that human TGCs can support HIV entry and  
118 integration, albeit inefficiently. Colonization of the human male germline could therefore lead  
119 to the vertical transmission of viral genes and ultimately to their endogenization in the next  
120 generations.

121

## 122 **Results**

### 123 **Isolation and characterization of primary human testicular germ cells (TGCs)**

124 We isolated fresh TGCs from the testes of uninfected donors displaying normal  
125 spermatogenesis and characterized them based on their ploidy profile (Fig. 1A, B) as well as  
126 expression of specific markers (Fig. 1C, D, E). As expected, three DNA content profiles were  
127 present in all TGCs preparations (n=9 donors) with a median value of 54% of n DNA  
128 spermatids (range 48-59%), 28% of 2n DNA spermatogonia and secondary spermatocytes  
129 (range 22-31%) and 20% of 4n DNA primary spermatocytes and mitotic spermatogonia  
130 (range 16-25%) (Fig. 1A, B). The germ cell marker DDX4 was detected in a median of 84%  
131 of TGCs (range 70-95%) (Fig. 1C, E). As expected, DDX4 did not label every germ cell  
132 because its expression is variable among germ cells, independently of their differentiation  
133 stage (38). TGCs with n, 2n and 4n DNA were DDX4+ with a median value of 80% (72-  
134 98%), 61% (40-95%) and 90% (68-97%), respectively (Fig. 1C). The early germ cell marker  
135 MAGEA4, which labels undifferentiated 2n DNA spermatogonia up to 4n DNA pre-leptotene  
136 primary spermatocyte (39), was detected in 40% (32-40%) of TGCs (n=3 donors), among  
137 which 37% (24-41%) of 2n DNA and 76% (72-86%) of 4n DNA cells (Fig.1C and E). The  
138 purity of TGCs preparations was systematically > 94%, as determined using somatic cell

139 markers HLA Class I (median 1%, range 0,4-4%) and vimentin (median 2%, range 1-6%) as  
140 well as pan-leukocytes marker CD45 (median 1%, range 0-4%) (Fig. 1D, E).

141

#### 142 **HIV binds to TGCs that express alternative receptors on their surface**

143 We first determined whether HIV can attach to TGCs by using the well characterized R5  
144 macrophage-tropic HIV-1<sub>SF162</sub> and X4 HIV-1<sub>IIIB</sub> strains (Fig.2). Dose-dependent binding to  
145 TGCs was observed for both strains (Fig.2A). Pronase treatment effectively removed bound  
146 HIV-1, indicating that the majority of the attached virions remained at the cell surface  
147 (Fig.2A). Similar findings were observed for a primary R5 non-macrophage tropic isolate and  
148 a primary R5X4 HIV-1 strain (Fig. 2B). Incubation of TGCs with a protease prior to viral  
149 exposure decreased HIV-1 p24 detection in cell lysates by a median of 97% (range 81-100%),  
150 indicating that cellular proteins mediated HIV-1 attachment to TGCs (Fig. 2C).

151 We next explored the expression of candidate receptors for HIV on the cell surface of TGCs  
152 (Fig. 3A, B). In agreement with our previous immunohistochemistry data (27), TGCs did not  
153 express the main HIV receptor CD4 (Fig. 3A, B). The chemokine HIV co-receptor CCR5 was  
154 detected in 4 out of 8 donors on the surface of a very low proportion of TGCs (median 5 %,  
155 range 2-12%), whereas CXCR4 was absent in all donors. The chemokine receptor CCR3 was  
156 expressed at the TGCs surface in all donors, with a median of 25,9% (14-45%) positive cells  
157 (Fig. 3A, B). The alternative HIV binding molecules CD206/mannose receptor,  
158 galactosylcerebroside, and heparan sulphate proteoglycans (HSPGs) were detected at the  
159 surface of TGCs from all donors, with a median of respectively 74% (51-90%), 77% (51-  
160 91%) and 7,1% (3-16%) positive cells (Fig. 3A,B). These receptors were expressed by TGCs  
161 irrespective of their DNA content (see representative profiles in Fig. 3A). Competition  
162 experiments with BSA-mannose, a ligand for CD206, induced a median reduction of virus  
163 attachment of 24% (range 16-29,1%) (Fig. 3C). In contrast, neutralizing antibodies against the

164 cellular glycolipid galactosylceramid had no effect on HIV attachment to TGCs (Fig. 3C), in  
165 agreement with the protease experiments. Heparin at 100 U/mL strongly inhibited the capture  
166 of HIV particles (median inhibition of 82%, range 79-86%) (Fig. 3C). The contribution of the  
167 viral envelope protein gp120 to binding was assessed using *env*-deleted pseudoviruses and  
168 anti-bodies against gp120 (Fig. 3D, E). In 4 independent experiments, the capture of HIV-1  
169 by TGCs was reduced by a median of 53,4% (range 52,6-54,7%) in the absence of *env* (Fig.  
170 3D), while Gp120 neutralizing antibodies reduced HIV binding to TGCs by a median of 29%  
171 (range 17-39%) (Fig. 3E), indicating that specific interactions of gp120 with cell surface  
172 receptors favored attachment.

173

#### 174 **TGCs support HIV-1 entry and integration**

175 We next investigated the ability of HIV to enter TGCs and process post-entry steps of viral  
176 replication. A major challenge for the study of primary TGCs *in vitro* is their low survival rate  
177 outside of the testis environment, since they require physical contacts and paracrine exchange  
178 with feeder somatic cells for their maintenance and development. To overcome this challenge,  
179 we set-up a co-culture of primary TGCs with human testicular somatic cells in a specific  
180 medium that allow long term maintenance of early germ cells (26). In this culture system,  
181 viability dyes showed over 80% of live TGCs after 12 days. After incubating freshly isolated  
182 TGCs with wild type HIV-1 R5 (SF162, BaL, JR-CSF) and X4 (IIIB) strains for 4 hours or  
183 overnight, HIV p24 was detected on the cell surface but not within the cells (Fig. 4A). Using a  
184 fluorescent HIV-1<sup>GFP-Vpr</sup> isolate, only rare entry events were visualized (Fig. 4B). To further  
185 dissect HIV interactions with testicular germ cells, we also analysed the well characterized  
186 human testicular germ cell line T-cam2, which displays characteristics of stem spermatogonia  
187 (40, 41), for HIV receptors expression and replication. Except for CXCR4, T-cam 2 cells  
188 displayed similar HIV receptor expression than primary TGCs (Fig. 4C) and HIV cell-free

189 entry was also inefficient (Fig. 4D and E). Because cell-associated infection is much more  
190 efficient than cell-free infection, and within the testis early TGCs are close to interstitial  
191 lymphocytes and macrophages, we investigated HIV entry and integration in TGCs incubated  
192 overnight with HIV-1 infected lymphocytes. Confocal microscopy showed DDX4-positive  
193 TGCs next to HIV-1-infected PBLs or Jurkat T cells (Fig. 4F) and revealed viral uptake of  
194 HIV-1 p24 by DDX4+ TGCs, some in division (Fig. 4G). Altogether, these results indicate  
195 that HIV-1 can enter primary TGCs in a cell-associated manner, whereas in our experimental  
196 model cell free infection was not readily detected.

197 To determine whether HIV DNA could integrate into the germ cell genome *in vitro*, freshly  
198 isolated TGCs were exposed to infected Jurkat T cells overnight, which were subsequently  
199 removed using anti-CD45 magnetic beads. TGCs were cultured for 3 to 7 days and viable  
200 cells sorted by flow cytometry, based on DDX4 and MAGEA4 expression and absence of  
201 leukocytes and somatic cell markers CD45, CD3 and HLA-DR detection (Fig. 5A, B). As a  
202 control, TGCs were mixed with infected Jurkat donor cells (2h contact) and processed without  
203 further incubation and culture, following the same protocol (magnetic beads and FACs  
204 sorting) as TGCs incubated ON with donor cells (Fig 5A). Following the cell selection  
205 procedure of cultured TGCs, most live germ cells were double positive for DDX4 and  
206 MAGEA4 (median 92%, range 82,6-99%), indicating TGCs in the pre-meiotic up to the early  
207 meiotic stage. In 3 independent experiments, sorted cultured germ cells were >99% positive  
208 for DDX4 and MAGEA4 (median 99.2, range 99-99.9%) and negative for immune cell  
209 markers CD45, CD3 and HLA-DR (representative profile in Fig. 5B). Alu-gag PCR  
210 performed on isolated TGCs demonstrated the presence of integrated HIV DNA in sorted  
211 cultured early germ cells from 3 out of 3 donors (Fig. 5C). Exposure of T-cam2 cells to Jurkat  
212 T cells infected with HIV-1 R5 and X4 strains also led to the detection of integrated HIV-1  
213 DNA after flow cytometry sorting of live cells negative for CD45 in 3 independent

214 experiments, whereas no integrated viral DNA was detected after cell-free infection (Fig. 5D).  
215 To bypass cell-free HIV entry restrictions, T-cam2 cells were infected with HIV-1  
216 pseudotyped with VSV envelope (VSV G). HIV DNA became readily measurable in T-cam2  
217 cells and its level was significantly decreased by RT inhibitor nevirapine, indicating active  
218 reverse-transcription of the viral genome (Fig. 5E). Integrated HIV-1 DNA was detected in T-  
219 cam2 cells' genome exposed to cell free HIV pseudotyped with VSV-G using Alu-gag PCR  
220 (Fig.5F). This detection was abrogated in the presence of nevirapine (Fig.5F).  
221 Altogether, these results indicate that isolated early germ cells can support low level of HIV-1  
222 DNA integration into their genome.

223

#### 224 **HIV-1/SIV DNA is present in TGCs *in vivo***

225 We next aimed to assess whether TGCs harboring HIV DNA are present *in vivo*. As  
226 mentioned, samples of testis tissue from HIV-infected men are extremely rare. Nevertheless  
227 we managed to have access to the testis of one HIV+ deceased patient. We screened for HIV  
228 DNA+ TGCs using next generation DNAscope *in situ* hybridization for HIV DNA combined  
229 with immunofluorescence detection of germ cell marker DDX4. Isolated DDX4+ germ cells  
230 harboring viral DNA were found within morphologically normal seminiferous tubules (Fig.  
231 5G). To investigate whether human TGCs are more restrictive to HIV infection than TGCs  
232 from non-human primates to SIV, we performed the same approach on the testis from one  
233 rhesus macaque and one African green monkey experimentally infected with SIV. In both the  
234 rhesus macaque and the African Green monkey, isolated HIV DNA+ TGCs were also  
235 observed (Fig. 5G). Overall, these results indicate that human TGCs can support low level of  
236 HIV replication up to DNA synthesis *in vivo*, similarly to their non-human primate  
237 counterparts, which could represent a way for HIV to become endogenous in the offspring.

238

239 **TGCs support low level of HIV replication**

240 Having shown that TGCs can harbour HIV DNA, we aimed to determine whether these cells  
241 could support HIV protein expression and virions production. Viral proteins expression in  
242 TGCs was analyzed following overnight exposure to Jurkat T cells infected with HIV-1  
243 bearing *nef-ires-GFP*. Nef-GFP was detected using confocal microscopy in primary DDX4+  
244 and MAGEA4+ TGCs after 9 to 12 days of culture (Fig. 6A). Similarly, low level of Nef-GFP  
245 was detected by flow cytometry in CD45-negative T-cam2 cells after cell-associated  
246 infection, and this detection abolished by pre-treatment of T-cam2 cells with RT-inhibitor  
247 nevirapine (Fig. 6B E). Following T-cam2 cells exposure to VSV-G pseudotyped HIV-1-  
248 bearing *nef-ires-GFP*, up to 9% of germ cells expressed Nef-GFP at day 5 post-infection,  
249 whereas less than 0.2 % of the cells were positive in the presence of nevirapine (Fig. 6C).  
250 Inhibitors of both HIV reverse-transcriptase (nevirapine) and integrase (raltegravir) similarly  
251 impaired the expression of intracellular p24 (Fig. 6D), demonstrating expression of viral  
252 proteins from *de novo* reverse transcribed and integrated virus. The release of infectious  
253 particles by T-cam2 cells was confirmed by the infection of permissive human PBLs with T-  
254 cam2 supernatants collected at day 5 and day 9 post-infection (Fig. 6E). Altogether, these  
255 results show that in addition to integration, early TGCs can support low level of viral  
256 production.

257

258 **Spermatogonia are enriched in HIV early co-factors compared with testicular somatic**  
259 **cells**

260 To further evaluate the permissiveness of TGCs to HIV replication post-entry, we compared  
261 the expression profiles of 335 factors that promote or inhibit HIV-1 life cycle post-entry  
262 among spermatogonia (SPG), spermatocytes (SPC) and spermatids (SPT) with that  
263 in two distinct testicular somatic cell types: testicular macrophages (TM), which

264 are permissive to HIV, and Sertoli cells (SC), which are not a target for HIV, using single cell  
265 RNA-sequencing data [42] (Table S1). As expected for an immune cell type, viral sensors ( $p=$   
266  $7.76e^{-6}$ ) and early inhibitors ( $p= 1.45e^{-2}$ ) were over represented in TM. This is in  
267 contrast to TGCs, among which sensors and early inhibitors were even depleted  
268 in SPC ( $p=6.26e^{-3}$  and  $2.59e^{-2}$ , respectively), whereas SC showed an intermediate profile in  
269 between that of TGCs and TM (Fig. 7). SPG were significantly enriched in late inhibitors ( $p=$   
270  $2.03e^{-2}$ ) although less so than TM ( $p= 1.33e^{-8}$ ), whereas SPC ( $p=1.95e^{-4}$ ) and SPT ( $p= 2.38e^{-5}$ )  
271 were depleted (Fig. 7). Interestingly, early co-factors spanning reverse transcription up to  
272 DNA integration steps were over-represented in SPG ( $p= 3.80e^{-4}$ ) but not in TM and SC, and  
273 tended to be depleted in SPT (albeit not significantly), suggesting a gradient of reduced  
274 permissiveness for HIV early replication steps as TGCs differentiate. The distribution  
275 frequency of late co-factors (most of them implicated in viral transcription) was comparable  
276 for all cell types (Fig. 7). Altogether, these data indicate that TGCs have overall lower innate  
277 sensing equipment and low proportion of early HIV inhibitors when compared with SC and  
278 TM. Due to their specific enrichment in early co-factors, SPG may represent a more  
279 permissive environment for HIV post-entry early steps up to viral DNA integration than late  
280 germ cells. Nevertheless, SPG are also enriched in late inhibitors, which could explain low  
281 viral production.

282

### 283 Discussion

284 Here we revealed that primary testicular germ cells can support HIV-1 genome integration  
285 and early viral proteins production upon contact with infected lymphocytes *in vitro*. In  
286 contrast, cell free virus infection did not lead to detectable viral entry despite HIV-1 binding  
287 to TGC and alternative receptors expression. DNAscope on the testis of one infected human  
288 and non-human primates demonstrated the presence of isolated HIV or SIV DNA+ TGCs.

289 Using the stem spermatogonia cell line T-cam2, we confirmed that viral integration occurred  
290 following cell-associated infection or after bypassing HIV-1 entry, and showed that these  
291 early germ cells can produce low level of infectious virions. Gene expression analysis of an  
292 array of factors affecting the viral life cycle showed that TGCs were not enriched in defense  
293 factors compared with testicular macrophages and Sertoli cells, and that spermatogonia were  
294 specifically enriched in co-factors involved in HIV post-entry life cycle up to integration.

295

296 While a number of viruses use ubiquitous receptors to attach and enter the cells, HIV virions  
297 require specific cellular receptors for infection. Although the main HIV receptor CD4 was  
298 absent, TGCs expressed on their surface CD206, GalCer and HSPGs, all previously showed  
299 to allow binding, entry or capture of a range of viruses including HIV in various cell types  
300 (42–49) . Ligands of HSPGs, and to a lesser extent of CD206, inhibited binding of cell free  
301 virions to TGCs, whereas despite its broad expression, GalCer was not involved, possibly  
302 because the detected isoform(s) were unable to bind gp120 (50). HIV binding to TGC only  
303 partly involved HIV envelope gp120, which could be due to HIV envelope-independent  
304 uptake by HSPGs, as previously described on other cells (51). These findings are comparable  
305 to that in spermatozoa (15, 43–45) and indicate that these receptors for viruses are retained on  
306 TGCs surface as they differentiate into spermatozoa. It implies that early TGCs located  
307 below the Sertoli cell tight junctions could act as Trojan horse, enabling the virions attached  
308 to their surface to cross the blood testis barrier as these cells progress to the seminal lumen  
309 during their differentiation. Bypassing the blood testis barrier could allow the virus to shelter  
310 from immune recognition by antibodies and immune cells, favoring viral reservoir  
311 establishment in the testis. It could also facilitate the release of viral particles into semen and  
312 their attachment to sperm.

313 In our experimental system, HIV entry and reverse transcription was not detected in primary  
314 TGCs exposed to cell-free wild type virus. In CD4-negative somatic cells, free viral particles  
315 entry has been reported *in vitro* but was overall inefficient, and viral internalization by  
316 vesicular uptake was essentially a dead end with respect to productive infection (46, 52–59).  
317 Despite free virus entry limitation, HIV-1 nucleic acids have been evidenced in HIV+  
318 individuals *in vivo* in specific CD4-negative cell types such as renal epithelial cells (60).  
319 Although the mechanism for HIV entry into these CD4 negative cells *in vivo* remains elusive,  
320 studies have suggested it may rely on cell-associated infection (54, 59, 61–63). Indeed, cell-  
321 to-cell contact between infected and non-infected target cells mediate the transfer of HIV-1 to  
322 recipient cells with much greater efficiency (100 to 1,000 times) than direct exposure of target  
323 cells to cell-free virus (64) and led to viral replication in a few CD4-negative cells, e.g. renal  
324 epithelial cells and astrocytes (54, 59, 63). In the testis of humans and non-human primates, T  
325 lymphocytes and interstitial macrophages infected with HIV/SIV are in close proximity to  
326 spermatogonia (28, 30, 36, 37), which are located at the basal compartment of the  
327 seminiferous epithelium and therefore not segregated by the blood/Sertoli cell testis barrier.  
328 Here we showed that co-culture of infected T cells and TGCs, as well as bypassing HIV entry  
329 steps with VSV envelope-pseudotyped HIV-1, led to HIV DNA integration into testicular  
330 germ cells' genome. Indeed, integrated viral DNA was measured in TGCs by Alu-gag PCR  
331 and was inhibited by a RT inhibitor, demonstrating the specificity of this detection. In  
332 addition, early viral protein synthesis was observed in labelled germ cells using confocal  
333 microscopy, an indicator of viral integration since unintegrated HIV-1 DNA is associated with  
334 transcriptional silencing (65). Finally, viral proteins detection in TGCs by flow cytometry was  
335 inhibited by both RT and integrase inhibitors.

336 Using next generation *in situ* hybridization, we aimed to determine whether TGCs are  
337 infected by HIV *in vivo*. Our results demonstrate the presence of isolated DDX4+ testicular

338 germ cells harboring HIV/SIV DNA in human, as well as in an experimental simian model of  
339 HIV infection (rhesus macaque) and a natural host for SIV (African Green monkey),  
340 indicating that the virus can proceed early replication steps in both human and simian TGCs  
341 *in vivo*. However, HIV and SIV DNA expression in TGCs was low, which might reflect  
342 requirement for cell-associated infection and low frequency of TGCs interactions with the  
343 infected leukocytes present in the interstitial tissue. Restriction factors could also be at play  
344 (see next paragraph). Due to the rarity of testis samples from infected individuals, we could  
345 not establish the frequency of HIV DNA detection in TGCs *in vivo*. However our *in vitro*  
346 results on TGCs together with our analysis of the testis from an HIV+ donor suggest it is  
347 likely to be low. The detection of HIV/SIV within differentiating germ cells distant from the  
348 base of the seminiferous tubules *in situ* could potentially result from clonal infection of early  
349 TGCs. Importantly, our data indicate that early TGCs remained viable in culture after viral  
350 entry, integration and protein expression, suggesting that viral integration was not detrimental  
351 to these cells. Clonal infection of the male germ line up to spermatozoa is suggested by  
352 reports of HIV DNA in a low percentage of ejaculated sperm (16–21, 23). Indeed  
353 spermatozoa do not support HIV entry, are transcriptionally silent and have a highly compact  
354 chromatin, thus preventing HIV replication steps. Patients' spermatozoa harboring viral DNA  
355 *in vivo* were reported to fertilize hamster ova and transfer HIV genome to early embryo (22),  
356 indicating that HIV did not impair their fertilization capacities.

357 The efficiency of HIV replication within a given cell type depends upon a fine balance  
358 between factors that positively (co-factors) or adversely (inhibitors) impact the virus life  
359 cycle, some of which are actively counteracted by HIV-1 proteins (e.g. APOBEC3G, BST2,  
360 SERINC5/3) (66). Using single-cell transcriptomic data of human testis, we analyzed the  
361 expression levels of 335 transcripts that affect HIV replication post-entry in isolated testicular  
362 germ cell populations and compared it with that in two somatic testicular cell types, an

363 immune cell type infected by HIV *in vivo* (testicular macrophages) and a non-immune cell  
364 type that is not infected by HIV (Sertoli cells) (27). Although we screened for a large number  
365 of known factors, we acknowledge that this analysis is not exhaustive and restricted to  
366 transcripts. We found that TGCs were not enriched in viral sensors or early inhibitors. In  
367 spermatogonia, except the vRNA sensor RIG-1 and its adaptor IRF3, genes encoding viral  
368 RNA, DNA or protein sensors were either not expressed (e.g. TLRs) or their necessary co-  
369 factors missing (e.g. IRF7, MyD88, STING), indicating restricted sensing equipment.  
370 Transcripts for a range of early HIV inhibitors including IFITM2 and 3 (fusion), PSG-L1  
371 (reverse-transcription), OAS (uncoating) and Mx2 (nuclear import) were also reduced in  
372 TGCs versus Sertoli cells and/or testicular macrophages. However, TRIM28 was well-  
373 expressed in TGCs compared with both Sertoli cells and testicular macrophages, which could  
374 explain limited HIV integration (Table S1). Interestingly, we recently demonstrated that  
375 human testicular germ cells were productively infected by Zika virus and that the infection  
376 did not impact their survival (26). In fact, testis antiviral responses were weak (26) and  
377 infected TGCs persisted in semen for prolonged duration (article in preparation). We and  
378 others also showed that rodent germ cells exposed to a range of viral stimuli did not produce  
379 interferon-stimulated antiviral proteins (reviewed in (1)). Altogether, these results suggest that  
380 aside their naturally protective testis environment (eg blood testis barrier and neighboring  
381 somatic cell types), testicular germ cells do not have strong canonical anti-viral equipment.  
382 Further studies are needed to decipher how TGCs respond to viral infections and whether they  
383 have evolved specific alternative protective mechanisms to restrict viral replication and its  
384 potentially deleterious effects.

385

386 Interestingly, early HIV co-factors spanning from reverse-transcription (e.g. DHX9 UBE2B  
387 and TRIAD3) to integration steps (LEDGF, INI1, NUP153) were observed at higher

388 frequency in spermatogonia as compared with testicular macrophages, Sertoli cells and late  
389 TGCs. We hypothesize that mitotic spermatogonia may therefore be more sensitive to HIV  
390 infection than late TGCs, all the more because their localization at the base of the  
391 seminiferous tubules could favor cell-to-cell infection by infected leukocytes, thus bypassing  
392 entry restriction. Because of their limited life span in culture, we could not determine whether  
393 spermatocytes and spermatids were less permissive to HIV replication than spermatogonia *in*  
394 *vitro*.

395

396 T-cam2 spermatogonia supported low level of HIV-1 replication up to the production of  
397 infectious viral particles, as demonstrated by the infection of PBMCs with infected T-cam2  
398 supernatants and by the inhibition of T-cam2 virus release by RT and integrase inhibitors. *In*  
399 *vivo*, viral RNA and proteins have been detected in a few TGCs within the testis of SIV-  
400 infected macaques (36, 37), suggesting viral production in a restricted number of cells. Our  
401 transcriptomic data analysis revealed that spermatogonia are enriched in a wide range of viral  
402 transcription inhibitors (e.g. HDAC1 and 2, negative elongation factor SPT5 and NELF-  
403 A/B/CD), which could restrict late viral replication and hence virions production. Altogether,  
404 our results support the consensus that male gametes are at best minor contributors to HIV  
405 horizontal transmission in comparison with productively infected leukocytes and free viral  
406 particles present in semen (35, 67, 68). Bearing in mind that a normal ejaculate contains  
407 millions of spermatozoa (WHO reference range 39-928 million), the chances for an individual  
408 to transmit HIV DNA to the genome of the offspring through oocyte fertilization with an  
409 HIV-infected sperm are naturally very low.

410

411 In conclusion, our study reveals that testicular early germ cells have the potential to support  
412 low level of HIV integration upon cell-associated infection. Such infection could represent a

413 way for HIV to integrate the germline and become endogenous in the future, as happened  
414 during human evolution for a number of retroviruses. Further studies are needed to determine  
415 the probability of this event at population level

416

## 417 **Materials and methods**

### 418 **Primary testicular germ cells (TGCs) isolation and culture**

419 Normal testes were obtained at autopsy or after orchidectomy from prostate cancer patients  
420 who had not received any hormone therapy. The procedure was approved by the National  
421 agency for biomedical research (authorization #PF S09-015) and CPP Ouest V local ethic  
422 committee (authorization #DC-2016-2783). Only testes displaying normal spermatogenesis,  
423 as assessed by transillumination, were used in this study. For receptor detection and HIV  
424 binding assay, testes were dissociated with tweezer, incubated in digesting medium (0.5  
425 mg/mL collagenase I, 75ug/mL DNase, 1ug/mL SBTI, PBS 1X) for 90min at 34°C under  
426 agitation (110 rpm) and then filtered (100µm). Seminiferous tubules were then mechanically  
427 dissociated to avoid trypsin usage, before cell filtration through 300µm and 100µm meshes in  
428 PBS containing DNase (40µg/mL). For testicular cells culture and entry assays, testicular  
429 tissues fragments were first incubated in digesting medium (2mg/mL hyaluronidase, 2mg/mL  
430 collagenase I, 20µg/mL in DMEM/F12) for 60 min at 37°C under agitation (110 rpm). After  
431 centrifugation, cell pellet was submitted to trypsin digestion (0.25%, 5mL/g, 20min at 37°C)  
432 before trypsin inactivation with FCS, then filtered (60µm), washed 3 times and cultured  
433 overnight in DMEM/F12 medium supplemented with 1X nonessential amino acids, 1X ITS  
434 (human insulin, human transferrin, and sodium selenite), 100U/mL penicillin, 100µg/mL  
435 streptomycin, 10%FCS (all reagents were from Sigma-Aldrich). Floating primary testicular  
436 germ cells were collected and cultured onto laminin (Sigma-Aldrich) treated dishes at a

437 density of 20,000 to 40,000 cells/cm<sup>2</sup> in supplemented StemPro-34 (Invitrogen) as described  
438 elsewhere (69).

439

#### 440 **Other cells and testis tissues**

441 Tcam-2 seminoma cell line (70)(kindly given by Dr Janet Shipley, The Institute of Cancer  
442 Research, London), and CCR5-expressing Jurkat (71) (provided by C. Goujon) were cultured  
443 in RPMI-1640 medium. Peripheral blood mononuclear cells (PBMCs) were prepared and  
444 cultured as previously described (72). 293T and positive control cells NP2-CD4, NP2-CCR5,  
445 NP2-CXCR4, GHOST-CCR3 and HT-29 cells were maintained in Dulbecco's Modified  
446 Eagles Medium (DMEM) supplemented with 10% fetal calf serum (FCS). All media were  
447 supplemented with 100U/mL penicillin, 100µg/mL streptomycin, 2mM L-glutamine and 10%  
448 FCS (all reagents from Sigma-Aldrich). Spermatozoa were obtained from healthy fertile  
449 volunteer donors with their informed consent (CPP Ouest V local ethic committee  
450 authorization #DC-2016-2783) using PureSperm gradient as instructed by manufacturer  
451 (Nidacon Laboratories AB, Gotheburg, Sweden). Human testicular tissue was obtained at  
452 autopsy from an HIV-1 infected man (donor 108, blood viral load at death 51 680 copies/mL)  
453 (73). NHP testicular tissues were collected at autopsy from an SIVagm+ African green  
454 monkey (*Chlorocebus sabaues*) euthanized 64 day post-infection for another study (blood  
455 viral load of 12 085 copies/mL) (74), and from a SIVmac251 Rhesus macaque euthanized at  
456 100 day post-infection (blood viral load > 10<sup>6</sup> copies/mL) (75).

457

#### 458 **Viruses and DNA constructs**

459 Wild type HIV-1 R5 macrophage-tropic (SF162, JR-CSF, BA-L) or X4 strains (IIIb) and  
460 primary isolates R5 non-macrophage tropic (ES X-2556-3, subtype B) or R5X4 (ESP-2196-2,  
461 subtype G) were obtained from the NIBSC (National Institute for Biological Standards and

462 Control Centralised Facility for AIDS Reagents) and viral stocks produced on PBMCs as  
463 previously described (72). The following viruses were generated by transiently transfecting  
464 293T cells with Lipofectamine 2000 (Invitrogen): 1) *env* deleted or HIV-1 *env* expressing  
465 pseudoviruses using transfer vector pHRsin-cppt-SEW (76), packaging pCMV8.2 (77), HxB2  
466 *env* pSVIII (78) (kindly provided by Stuart Neil, King's college, London, UK); 2) HIV-1<sup>GFP</sup>-  
467 <sup>Vpr</sup> viral particles, using pSG3Δ*env*, pcDNA3.1D/V5-His-TOPO-*env*<sub>SF162</sub>, *vpr*-*gfp* (79)(a kind  
468 gift from Christiane Moog, University of Strasbourg, France); 3) VSV G- pseudotyped HIV-1  
469 using full-length HIV-1 molecular clone pNL4-3 (80) or the R5-tropic pNL4-3 AD8  
470 derivative (81) and VSV-G envelope encoding plasmid (PT3343-5, Clontech); 4) VSV G-  
471 pseudotyped HIV-1 *nef*-ires-GFP using pBR\_NL4-3 IRES-eGFP (X4-tropic) or pBR\_NL4-3  
472 92TH014.12 IRES eGFP (R5 tropic) (82) (a kind gift from Frank Kirchhoff, Ulm University,  
473 Germany) and VSV-G envelope encoding plasmid (PT3343-5, Clontech). 293T cell  
474 supernatants were collected 3 days post-transfection, filtered using 0.45 µm membrane and  
475 stored at -80°C.

476

#### 477 **Flow cytometry for antigen detection and cell sorting**

478 Immunostaining of surface antigens was performed as previously described (83). The  
479 following antibodies were used: anti-CD45 (-PE or PC7 conjugated, HI30, BD Pharmingen),  
480 anti-HLA-ABC-PE (G46-2.6, BD Pharmingen) anti-Vimentin (EPR3776, 1µg/mL,  
481 Epitomics), anti-DDX4 (Rabbit polyclonal, 5µg/mL, Abcam), anti-MAGEA4 (clone 57B,  
482 4µg/mL) (39), anti-CD4 (ARP337, 10µg/mL), anti-CXCR4 (ARP3101 12G5, 10µg/mL)  
483 (both from EVA/MRC, NIBSC), anti-CCR5 (45549, 10µg/mL, R&D), anti-CCR3 (61828,  
484 5µg/mL, R&D), anti-GalactosylCeramide (mGalC, 10µg/mL, Millipore), anti-Heparan  
485 Sulfate-ProteoGlycans (10E4, 5µg/mL, Seikagaku corporation) and anti-p24 gag RD1 (KC57,  
486 Beckman coulter). PE conjugated anti-mouse or anti-rabbit Ig (Jackson Immunoresearch)

487 were used as secondary antibodies. Control isotype antibodies were used as negative controls,  
488 except for HSPGs where cells were pretreated or not with pronase (3,5mg/mL, Roche) and  
489 then subjected to immunostaining. The expression of Mannose Receptor (MR) was analyzed  
490 as previously described (15). Cellular DNA content was determined using DRAQ5 (20uM,  
491 Biostatus Limited). FACScalibur flow cytometer (Becton Dickinson, Franklin Lakes, USA)  
492 and CELLQuestPro Software were used for acquisition and analysis.

493 For cell sorting, TGCs were stained with the fixable viability stain FVS450 (BD Biosciences),  
494 as recommended by the supplier before fixation in 1,5% paraformaldehyde. Cells were then  
495 labelled using DDX4 anti-rabbit-PE antibodies, CD45-PC7 Ab (clone J33, 1/15, Beckman  
496 Coulter), CD3-BV510 Ab (clone HIT3a, 1µg/mL, BD Biosciences), HLA-DR-BV510 Ab  
497 (clone G46-6, 7µg/mL, BD Biosciences) and MAGEA4 Ab (clone 57B, 4µg/mL) (39)  
498 previously coupled to Alexa Fluor 647 using Zenon labeling kit (Molecular Probes). Matched  
499 isotype antibodies were used as negative controls. Cells negative for CD45, CD3, HLA-DR  
500 and positive for DDX4 and/or MAGEA4 were sorted using FACSARIA flow cytometer  
501 (Becton Dickinson, Franklin Lakes, USA) connected to the DIVA software. For Tcam-2,  
502 CD45-PC7 antibody was used for CD45 negative T-cam2 cell sorting.

503

#### 504 **Binding assay**

505 The binding assay was performed as previously described (15), with some modifications.  
506 Briefly, cells were incubated with indicated HIV-1 strains (25 or 75 ng p24 per 10<sup>6</sup> cells) in a  
507 final volume of 150µL of medium and incubated for 2 hours at 37°C in RPMI-1640 2,5%  
508 FCS. Cells were then thoroughly washed, lysed and the p24 content determined by ELISA.  
509 When indicated, the assay was performed on cells exposed to Pronase (3,5mg/ml) or using  
510 virus pre-exposed to 1 to 100 U/mL heparin (Sigma-Aldrich). The role of mannose receptor  
511 was evaluated by incubating cells with HIV-1 in the presence of 100µg/mL BMA (Sigma-

512 Aldrich) or 100µg/mL bovine serum albumin (BSA) as control. Neutralization assays were  
513 performed by pre-incubating cells with anti-GalactosylCeramide antibody (mGalC, 10µg/mL,  
514 Millipore 10µg/mL, 30 min at 4°C) or viral inoculum with monoclonal antibody against HIV-  
515 1 gp120 (1-2µg/mL, clone F105, AIDS Reagents, NIBSC, 30 min at 37°C). Matched isotype  
516 antibodies were used as negative controls. Controls for nonspecific viral attachment were  
517 systematically performed by incubating viral inoculum in the absence of cells. In all  
518 experiments, each condition was performed in duplicate and residual p24 level deduced.

519

### 520 **Cell infection**

521 TGCs, Tcam-2 and Jurkat cells were infected with 200ng p24/10<sup>6</sup> cells of the indicated virus  
522 as previously described (83) and cultured with or without 37,5µM nevirapin (non-nucleosidic  
523 reverse-transcriptase inhibitor) or 100nM raltegravir (integrase inhibitor) (both from AIDS  
524 Reagents, NIBSC), as specified. For cell-associated infection, Jurkat donor cells were infected  
525 with the indicated VSV-G pseudotyped HIV NL4-3 strain. TGCs or T-cam2 were incubated  
526 for 18h with infected Jurkat cells (40 to 80% positive for HIV-1 Gag or GFP). Donor cells  
527 were then removed by positive selection of CD45+ cells (CD45 microbeads kit, Miltenyi  
528 Biotec) (TGCs) or pipetting (Tcam-2) and target cells put in culture. GFP content was  
529 analysed at the indicated time points in DDX4 positive cells by confocal microscopy (TGCs)  
530 or by flow cytometry in CD45 negative Tcam-2 cells. For integrated viral DNA  
531 quantification, TGCs and Tcam-2 were further purified by FACS sorting as described above  
532 (see Flow cytometry and cell sorting).

533

### 534 **Confocal microscopy for viral entry**

535 Germ cells were pre-labelled with 10uM CFSE or CellTrace Violet (Invitrogen) before being  
536 exposed to free viral particles overnight and treated with 0.25% trypsin-EDTA (Sigma-

537 Aldrich) for 5 min at 37°C post-infection to remove virions attached to the cell surface. Cells  
538 were loaded onto polylysine-coated coverslips, fixed in 4% para-formaldehyde, washed in  
539 PBS and incubated in a blocking/permeabilizing solution (0.3M Glycine, 0.05% Triton-X, 3%  
540 BSA, 1X PBS) for 30 min at RT. Cells were then stained with the following antibodies:  
541 mouse monoclonal anti-p24 (183-H12-5C, EVA, NIBSC), rabbit anti-DDX4 (5µg/mL,  
542 Abcam), mouse anti-MageA4 (clone 57B, 4µg/mL) (39), CD45-Alexa-fluor 647 (J.33 clone,  
543 Beckman coulter). Anti-mouse Alexa-fluor 555 (Thermo Fisher Scientific), anti-rabbit Alexa-  
544 fluor 488 (Thermo Fisher Scientific) and Alexa-fluor 647 (Jackson Immunoresearch) were  
545 used as secondary antibodies. Isotype control antibodies or mock infected cells were used as  
546 controls. Nuclei were stained either with 10 µM DRAQ5 (Biostatus) or with DAPI (Molecular  
547 Probes), and slides mounted with Prolong Gold Antifade mountant (Molecular Probes).  
548 Images were acquired with the SP8 confocal system microscope (objective 60X, Z-step 0.3 to  
549 0.5µm intervals) (Leica) connected to LAS software and analyzed with Fiji software.

550

#### 551 **Real-Time PCR for HIV-1 DNA**

552 Intracellular HIV-1 DNA was measured as previously described (73). Input virus was treated  
553 with benzonase (500U/mL, Sigma-Aldrich) before cell exposure to reduce nucleic acid  
554 contamination in the viral stock. Cells infected in the presence of the RT inhibitor nevirapin  
555 (37,5µM) were used to discriminate DNA originated from input viruses. Integrated HIV DNA  
556 was quantified as previously described using Alu-gag PCR assay (84).

557

#### 558 **Next generation *in situ* hybridization (DNAScope)**

559 DNAScope was used for the detection of viral DNA for both HIV and SIV, as previously  
560 described (75). To immunophenotype the cells containing vDNA, DNAScope detection by  
561 Tyramide Signal Amplification (TSA™) Plus Cy3.5 was combined with immunofluorescence

562 targeting cell markers using rabbit polyclonal anti-DDX4 (1:500; Abcam) for TGC and mouse  
563 monoclonal anti-CD4 (1:100; clone 1F6, Vector) for T-lineage cells. 4 to 6 5 $\mu$ m sections were  
564 run per sample. An average of 90982mm<sup>2</sup> of tissue area was screen to find positive event.  
565 Fluorescent slides mounted with Prolong<sup>®</sup> Gold (Invitrogen) were imaged on an Olympus  
566 FV10i confocal microscope using a 60x phase contrast oil-immersion objective (NA 1.35) and  
567 applying a sequential mode to separately capture the fluorescence from the different  
568 fluorochromes at an image resolution of 1024 x 1024 pixels.

569

#### 570 **p24 ELISA and infectivity assay**

571 p24 concentrations in T-cam2 cells were measured by ELISA (Innogenetics, according to  
572 manufacturer's instructions) and the infectivity of viral particles determined through PBMCs  
573 exposure to T-cam2 cell supernatants for 4 h, with p24 quantification at the indicated time  
574 post-infection.

575

#### 576 **Analysis of single-cell RNA-sequencing data**

##### 577 *Data processing*

578 Single-cell RNA-sequencing data of human adult testicular cells (85) were recovered from the  
579 ReproGenomics Viewer (86, 87) and processed using the AMEN software (88). Briefly, out  
580 of the 23'109 genes measured in this experiment, only those with an average expression level  
581 ( $\log_2[\text{count}+1]$ ) of at least 1 in a least one cell population and a fold-change of at least 2  
582 between at least two cell populations were considered as being differentially-expressed.  
583 Selected genes were further classified according to their peak expression in testicular  
584 macrophages (Cell population tM $\phi$  in the initial publication of (85)), in Sertoli cells, in  
585 spermatogonia (cell populations SSC1, SSC2, differentiating and differentiated SPG in the  
586 original publication), in primary or secondary spermatocytes (cell populations L1, L2, L3, Z,

587 P, D and SPC7 in the original publication) or in round or elongated spermatids (Cell  
588 population S1 to S4 in the original publication). The consistency of the results was controlled  
589 by comparing expression profiles of all selected genes to those obtained by Hermann *et al.*  
590 (89).

#### 591 *Enrichment analysis*

592 A list of known factors involved in HIV life cycle post-entry was retrieved from the literature  
593 (Table S1). These were annotated as “Early Co-factors” (79 genes), “Late Co-factors” (28  
594 genes), “Sensors” (15 genes), “Early inhibitors” (28 genes) or “Late inhibitors” (185 genes)  
595 according to their demonstrated roles. The over- and under-representation of these factors  
596 among clusters of differentially-expressed genes was then evaluated with a hypergeometric  
597 test, while the false discovery rate was controlled by adjusting resulting p-values using the  
598 Benjamini and Hochberg method (90).

599

#### 600 **Statistical analysis**

601 Statistical analyses were performed using commercially available software (GraphPadPrism  
602 6, GraphPad Software, Inc., La Jolla, California, USA). Data were analysed with non-  
603 parametric Friedman-Dunn's test or Mann Whitney test, as indicated in figure legends. Values  
604 were considered significant when  $P < 0.05$ . Statistical analyses performed on single-cell RNA-  
605 sequencing data are described above in the relevant section.

606

607

#### 608 **ACKNOWLEDGEMENTS**

609 This project received funding from Inserm, ANRS, Sidaction, CAPES-COFECUB and was  
610 funded in part with Federal funds from the National Cancer Institute, National Institutes of  
611 Health, under Contract No. HHSN261200800001E. Experiments were conducted in part on

612 L3, MRic, H2P2 and flow cytometry platforms at Biosit federative structure (Univ Rennes,  
613 CNRS, Inserm, BIOSIT [(Biologie, Santé, Innovation Technologique de Rennes)] - UMS  
614 3480, US\_S018). The content of this publication does not necessarily reflect the views or  
615 policies of the Department of Health and Human Services, nor does mention of trade names,  
616 commercial products, or organizations imply endorsement by the U.S. Government.

617

618

## 619 REFERENCES

- 620 1. Le Tortorec A, Matusali G, Mahé D, Aubry F, Mazaud-Guittot S, Houzet L, Dejuq-  
621 Rainsford N. 2020. From Ancient to Emerging Infections: The Odyssey of Viruses in  
622 the Male Genital Tract. *Physiol Rev* physrev.00021.2019.
- 623 2. Griffiths DJ. 2001. Endogenous retroviruses in the human genome sequence. *Genome*  
624 *Biol.* BioMed Central.
- 625 3. Feschotte C, Gilbert C. 2012. Endogenous viruses: insights into viral evolution and  
626 impact on host biology. *Nat Rev Genet* 13:283–296.
- 627 4. Tarlinton RE, Meers J, Young PR. 2006. Retroviral invasion of the koala genome.  
628 *Nature* 442:79–81.
- 629 5. Kassiotis G, Stoye JP. 2016. Immune responses to endogenous retroelements: taking  
630 the bad with the good. *Nat Rev Immunol* 16:207–219.
- 631 6. Jern P, Coffin JM. 2008. Effects of Retroviruses on Host Genome Function. *Annu Rev*  
632 *Genet* 42:709–732.
- 633 7. Katzourakis A, Tristem M, Pybus OG, Gifford RJ. 2007. Discovery and analysis of the  
634 first endogenous lentivirus. *Proc Natl Acad Sci U S A* 104:6261–5.
- 635 8. Gifford RJ, Katzourakis A, Tristem M, Pybus OG, Winters M, Shafer RW. 2008. A  
636 transitional endogenous lentivirus from the genome of a basal primate and implications  
637 for lentivirus evolution. *Proc Natl Acad Sci U S A* 105:20362–7.
- 638 9. Gilbert C, Maxfield DG, Goodman SM, Feschotte C, Ment Gilbert C, Maxfield DG,  
639 Goodman SM, Dric Feschotte C. 2009. Parallel germline infiltration of a lentivirus in  
640 two Malagasy lemurs. *PLoS Genet* 5:e1000425.
- 641 10. Keckesova Z, Ylinen LMJ, Towers GJ, Gifford RJ, Katzourakis A. 2009. Identification  
642 of a RELIK orthologue in the European hare (*Lepus europaeus*) reveals a minimum age  
643 of 12 million years for the lagomorph lentiviruses. *Virology* 384:7–11.
- 644 11. Han G-Z, Worobey M. 2012. Endogenous lentiviral elements in the weasel family  
645 (Mustelidae). *Mol Biol Evol* 29:2905–8.
- 646 12. Hron T, Fábryová H, Pačes J, Elleder D. 2014. Endogenous lentivirus in Malayan  
647 colugo (*Galeopterus variegatus*), a close relative of primates. *Retrovirology* 11:84.
- 648 13. Houzet L, Matusali G, Dejuq-Rainsford N. 2014. Origins of HIV-infected leukocytes  
649 and virions in semen. *J Infect Dis* 210:S622–S630.
- 650 14. Houzet L, Pérez-Losada M, Matusali G, Deleage C, Dereuddre-Bosquet N, Satie A-PP,  
651 Aubry F, Becker E, Jégou B, Le Grand R, Keele BF, Crandall KA, Dejuq-Rainsford  
652 N, Perez-Losada M, Matusali G, Deleage C, Dereuddre-Bosquet N, Satie A-PP, Aubry  
653 F, Becker E, Jégou B, Le Grand R, Keele BF, Crandall KA, Dejuq-Rainsford N,  
654 Pérez-Losada M, Matusali G, Deleage C, Dereuddre-Bosquet N, Satie A-PP, Aubry F,  
655 Becker E, Jégou B, Le Grand R, Keele BF, Crandall KA, Dejuq-Rainsford N. 2018.  
656 Seminal Simian Immunodeficiency Virus in Chronically Infected *Cynomolgus*  
657 *Macaques* Is Dominated by Virus Originating from Multiple Genital Organs. *J Virol*  
658 92:e00133-18.
- 659 15. Ceballos A, Remes Lenicov F, Sabatte J, Rodriguez Rodrigues C, Cabrini M, Jancic C,  
660 Raiden S, Donaldson M, Agustin Pasqualini Jr. R, Marin-Briggiler C, Vazquez-Levin  
661 M, Capani F, Amigorena S, Geffner J, Sabatté J, Rodríguez Rodríguez C, Cabrini M,  
662 Jancic C, Raiden S, Donaldson M, Agustín Pasqualini R, Marin-Briggiler C, Vazquez-  
663 Levin M, Capani F, Amigorena S, Geffner J, Sabatte J, Rodriguez Rodrigues C,  
664 Cabrini M, Jancic C, Raiden S, Donaldson M, Agustin Pasqualini Jr. R, Marin-  
665 Briggiler C, Vazquez-Levin M, Capani F, Amigorena S, Geffner J, Sabatté J,  
666 Rodríguez Rodríguez C, Cabrini M, Jancic C, Raiden S, Donaldson M, Agustín  
667 Pasqualini R, Marin-Briggiler C, Vazquez-Levin M, Capani F, Amigorena S, Geffner J.  
668 2009. Spermatozoa capture HIV-1 through heparan sulfate and efficiently transmit the

- 669 virus to dendritic cells. *J Exp Med* 206:2717–2733.
- 670 16. Scofield VL, Rao B, Broder S, Kennedy C, Wallace M, Graham B, Poiesz BJ. 1994.
- 671 HIV interaction with sperm. *AIDS* 8:1733–6.
- 672 17. Bagasra O, Farzadegan H, Seshamma T, Oakes JW, Saah A, Pomerantz RJ. 1994.
- 673 Detection of HIV-1 proviral DNA in sperm from HIV-1-infected men. *AIDS* 8:1669–
- 674 1674.
- 675 18. Dulioust E, Tachet A, De Almeida M, Finkielsztejn L, Rivalland S, Salmon D, Sicard
- 676 D, Rouzioux C, Jouannet P. 1998. Detection of HIV-1 in seminal plasma and seminal
- 677 cells of HIV-1 seropositive men. *J Reprod Immunol* 41:27–40.
- 678 19. Marina S, Marina F, Alcolea R, Expósito R, Huguet J, Nadal J, Vergés A. 1998.
- 679 Human immunodeficiency virus type 1–serodiscordant couples can bear healthy
- 680 children after undergoing intrauterine insemination. *Fertil Steril* 70:35–39.
- 681 20. Leruez-Ville M, de Almeida M, Tachet A, Dulioust E, Guibert J, Mandelbrot L,
- 682 Salmon D, Jouannet P, Rouzioux C. 2002. Assisted reproduction in HIV-1-
- 683 serodifferent couples. *AIDS* 16:2267–2273.
- 684 21. Muciaccia B, Corallini S, Vicini E, Padula F, Gandini L, Liuzzi G, Lenzi A, Stefanini
- 685 M. 2007. HIV-1 viral DNA is present in ejaculated abnormal spermatozoa of
- 686 seropositive subjects. *Hum Reprod* 22:2868–2878.
- 687 22. Wang D, Li L-BB, Hou Z-WW, Kang X-JJ, Xie Q-DD, Yu XJ, Ma M-FF, Ma B-LL,
- 688 Wang Z-SS, Lei Y, Huang T-HH. 2011. The integrated HIV-1 provirus in patient
- 689 sperm chromosome and its transfer into the early embryo by fertilization. *PLoS One*
- 690 6:e28586.
- 691 23. Baccetti B, Benedetto A, Burrini AG, Collodel G, Ceccarini EC, Crisà N, Di Caro A,
- 692 Estenoz M, Garbuglia AR, Massacesi A, Piomboni P, Renieri T, Solazzo D. 1994.
- 693 HIV-particles in spermatozoa of patients with AIDS and their transfer into the oocyte. *J*
- 694 *Cell Biol* 127:903–14.
- 695 24. Barboza JM, Medina H, Doria M, Rivero L, Hernandez L, Joshi N V. 2004. Use of
- 696 atomic force microscopy to reveal sperm ultrastructure in HIV-patients on highly active
- 697 antiretroviral therapy. *Arch Androl* 50:121–9.
- 698 25. Cardona-Maya W, Velilla P, Montoya C, Cadavid A, Rugeles M. 2009. Presence of
- 699 HIV-1 DNA in Spermatozoa from HIV-Positive Patients: Changes in the Semen
- 700 Parameters. *Curr HIV Res* 7:418–424.
- 701 26. Matusali G, Houzet L, Satie A-P, Mahé D, Aubry F, Couderc T, Frouard J, Bourgeau
- 702 S, Bensalah K, Lavoué S, Joguet G, Bujan L, Cabié A, Avelar G, Lecuit M, Tortorec A
- 703 Le, Dejuq-Rainsford N. 2018. Zika virus infects human testicular tissue and germ
- 704 cells. *J Clin Invest* 128:4697–4710.
- 705 27. Roulet V, Satie A-PP, Ruffault A, Le Tortorec A, Denis H, Guist’hau O, Patard J-JJ,
- 706 Rioux-Leclercq N, Gicquel J, Jégou B, Dejuq-Rainsford N, Jegou B, Dejuq-Rainsford
- 707 N. 2006. Susceptibility of human testis to human immunodeficiency virus-1 infection
- 708 in situ and in vitro. *Am J Pathol* 169:2094–103.
- 709 28. Pudney J, Anderson D. 1991. Orchitis and human immunodeficiency virus type 1
- 710 infected cells in reproductive tissues from men with the acquired immune deficiency
- 711 syndrome. *Am J Pathol* 139:149–60.
- 712 29. Jenabian M-A, Costiniuk CT, Mehraj V, Ghazawi FM, Fromentin R, Brousseau J,
- 713 Brassard P, Bélanger M, Ancuta P, Bendayan R, Chomont N, Routy J-P, Orchid study
- 714 group. 2016. Immune tolerance properties of the testicular tissue as a viral sanctuary
- 715 site in ART-treated HIV-infected adults. *AIDS* 30:2777–2786.
- 716 30. Muciaccia B, Filippini A, Ziparo E, Colelli F, Baroni CD, Stefanini M. 1998.
- 717 Testicular germ cells of HIV-seropositive asymptomatic men are infected by the virus.
- 718 *J Reprod Immunol* 41:81–93.

- 719 31. França LR, Auharek SA, Hess RA, Dufour JM, Hinton BT. 2012. Blood-tissue  
720 barriers: morphofunctional and immunological aspects of the blood-testis and blood-  
721 epididymal barriers. *Adv Exp Med Biol* 763:237–59.
- 722 32. Nuovo GJ, Becker J, Simsir A, Margiotta M, Khalife G, Shevchuk M. 1994. HIV-1  
723 nucleic acids localize to the spermatogonia and their progeny. A study by polymerase  
724 chain reaction in situ hybridization. *Am J Pathol* 144:1142–8.
- 725 33. Shevchuk MM, Nuovo GJ, Khalife G. 1998. HIV in testis: quantitative histology and  
726 HIV localization in germ cells. *J Reprod Immunol* 41:69–79.
- 727 34. Pudney J, Nguyen H, Xu C, Anderson DJ. 1999. Erratum to “Microscopic evidence  
728 against HIV-1 infection of germ cells or attachment to sperm”: [*J. Reprod. Immun.* 41  
729 (1998) 105–125]. *J Reprod Immunol* 44:57–77.
- 730 35. Le Tortorec A, Dejucq-Rainsford N. 2009. HIV infection of the male genital tract--  
731 consequences for sexual transmission and reproduction. *Int J Androl* 32:1–12.
- 732 36. Le Tortorec A, Le Grand R, Denis H, Satie A-P, Mannioui K, Roques P, Maillard A,  
733 Daniels S, Jégou B, Dejucq-Rainsford N. 2008. Infection of semen-producing organs  
734 by SIV during the acute and chronic stages of the disease. *PLoS One* 3:e1792.
- 735 37. Shehu-Xhilaga M, Kent S, Batten J, Ellis S, Van der Meulen J, O’Bryan M, Cameron  
736 PU, Lewin SR, Hedger MP. 2007. The testis and epididymis are productively infected  
737 by SIV and SHIV in juvenile macaques during the post-acute stage of infection.  
738 *Retrovirology* 4:7.
- 739 38. Zeeman A-M, Stoop H, Boter M, Gillis AJM, Castrillon DH, Oosterhuis JW,  
740 Looijenga LHJ. 2002. VASA Is a Specific Marker for Both Normal and Malignant  
741 Human Germ Cells. *Lab Invest* 82:159–166.
- 742 39. Aubry F, Satie AP, Rioux-Leclercq N, Rajpert-De Meyts E, Spagnoli GC, Chomez P,  
743 De Backer O, Jégou B, Samson M. 2001. MAGE-A4, a germ cell specific marker, is  
744 expressed differentially in testicular tumors. *Cancer* 92:2778–2785.
- 745 40. de Jong J, Stoop H, Gillis AJM, Hersmus R, van Gurp RJHLM, van de Geijn G-JM,  
746 van Drunen E, Beverloo HB, Schneider DT, Sherlock JK, Baeten J, Kitazawa S, van  
747 Zoelen EJ, van Roozendaal K, Oosterhuis JW, Looijenga LHJ. 2008. Further  
748 characterization of the first seminoma cell line TCam-2. *Genes, Chromosom Cancer*  
749 47:185–196.
- 750 41. Young JC, Jaiprakash A, Mithraprabhu S, Itman C, Kitazawa R, Looijenga LHJ,  
751 Loveland KL. 2011. TCam-2 seminoma cell line exhibits characteristic foetal germ cell  
752 responses to TGF-beta ligands and retinoic acid. *Int J Androl* 34:e204–e217.
- 753 42. Connell BJ, Lortat-Jacob H. 2013. Human Immunodeficiency Virus and Heparan  
754 Sulfate: From Attachment to Entry Inhibition. *Front Immunol* 4:385.
- 755 43. Bandivdekar AH, Velhal SM, Raghavan VP. 2003. Identification of CD4-independent  
756 HIV Receptors on Spermatozoa. *Am J Reprod Immunol* 50:322–327.
- 757 44. Cardona-Maya W, Lopez-Herrera A, Velilla-Hernandez P, Rugeles MT, Cadavid AP.  
758 2006. The Role of Mannose Receptor on HIV-1 Entry into Human Spermatozoa. *Am J*  
759 *Reprod Immunol* 55:241–245.
- 760 45. Fanibunda SE, Velhal SM, Raghavan VP, Bandivdekar AH. 2008. CD4 Independent  
761 Binding of HIV gp120 to Mannose Receptor on Human Spermatozoa. *J Acquir*  
762 *Immune Defic Syndr* 48:389–397.
- 763 46. Liu Y, Liu H, Kim BO, Gattone VH, Li J, Nath A, Blum J, He JJ. 2004. CD4-  
764 independent infection of astrocytes by human immunodeficiency virus type 1:  
765 requirement for the human mannose receptor. *J Virol* 78:4120–33.
- 766 47. Harouse JM, Bhat S, Spitalnik SL, Laughlin M, Stefano K, Silberberg DH, Gonzalez-  
767 Scarano F. 1991. Inhibition of entry of HIV-1 in neural cell lines by antibodies against  
768 galactosyl ceramide. *Science* (80- ) 253:320–323.

- 769 48. Riblett AM, Blomen VA, Jae LT, Altamura LA, Doms RW, Brummelkamp TR,  
770 Wojcechowskyj JA. 2016. A Haploid Genetic Screen Identifies Heparan Sulfate  
771 Proteoglycans Supporting Rift Valley Fever Virus Infection. *J Virol* 90:1414–1423.
- 772 49. Gao H, Lin Y, He J, Zhou S, Liang M, Huang C, Li X, Liu C, Zhang P. 2019. Role of  
773 heparan sulfate in the Zika virus entry, replication, and cell death. *Virology* 529:91–  
774 100.
- 775 50. Gadella B., Hammache D, Piéroni G, Colenbrander B, van Golde LM., Fantini J. 1998.  
776 Glycolipids as potential binding sites for HIV: topology in the sperm plasma membrane  
777 in relation to the regulation of membrane fusion. *J Reprod Immunol* 41:233–253.
- 778 51. Vidricaire G, Gauthier S, Tremblay MJ. 2007. HIV-1 Infection of Trophoblasts Is  
779 Independent of gp120/CD4 Interactions but Relies on Heparan Sulfate Proteoglycans. *J*  
780 *Infect Dis* 195:1461–1471.
- 781 52. Vijaykumar TS, Nath A, Chauhan A. 2008. Chloroquine mediated molecular tuning of  
782 astrocytes for enhanced permissiveness to HIV infection. *Virology* 381:1–5.
- 783 53. Chauhan A, Mehla R, Vijayakumar TS, Handy I. 2014. Endocytosis-mediated HIV-1  
784 entry and its significance in the elusive behavior of the virus in astrocytes. *Virology*  
785 456–457:1–19.
- 786 54. Luo X, He JJ. 2015. Cell–cell contact viral transfer contributes to HIV infection and  
787 persistence in astrocytes. *J Neurovirol* 21:66–80.
- 788 55. Vidricaire G, Tremblay MJ. 2007. A Clathrin, Caveolae, and Dynamin-independent  
789 Endocytic Pathway Requiring Free Membrane Cholesterol Drives HIV-1  
790 Internalization and Infection in Polarized Trophoblastic Cells. *J Mol Biol* 368:1267–  
791 1283.
- 792 56. Khatua AK, Taylor HE, Hildreth JEK, Popik W. 2010. Non-productive HIV-1  
793 infection of human glomerular and urinary podocytes. *Virology* 408:119–27.
- 794 57. Dezzutti CS, Guenther PC, Cummins, Jr. JE, Cabrera T, Marshall JH, Dillberger A,  
795 Lal RB. 2001. Cervical and Prostate Primary Epithelial Cells Are Not Productively  
796 Infected but Sequester Human Immunodeficiency Virus Type 1. *J Infect Dis* 183:1204–  
797 1213.
- 798 58. Dorosko SM, Connor RI. 2010. Primary human mammary epithelial cells endocytose  
799 HIV-1 and facilitate viral infection of CD4+ T lymphocytes. *J Virol* 84:10533–10542.
- 800 59. Blasi M, Balakumaran B, Chen P, Negri DRM, Cara A, Chen BK, Klotman ME. 2014.  
801 Renal epithelial cells produce and spread HIV-1 via T-cell contact. *AIDS* 28:2345–53.
- 802 60. Bruggeman LA, Ross MD, Tanji N, Cara A, Dikman S, Gordon RE, Burns GC,  
803 D’Agati VD, Winston JA, Klotman ME, Klotman PE. 2000. Renal epithelium is a  
804 previously unrecognized site of HIV-1 infection. *J Am Soc Nephrol* 11:2079–87.
- 805 61. Chen P, Chen BK, Mosoian A, Hays T, Ross MJ, Klotman PE, Klotman ME. 2011.  
806 Virological synapses allow HIV-1 uptake and gene expression in renal tubular  
807 epithelial cells. *J Am Soc Nephrol* 22:496–507.
- 808 62. Russell RA, Chojnacki J, Jones DM, Johnson E, Do T, Eggeling C, Padilla-Parra S,  
809 Sattentau QJ. 2017. Astrocytes Resist HIV-1 Fusion but Engulf Infected Macrophage  
810 Material. *Cell Rep* 18:1473–1483.
- 811 63. Li G-H, Anderson C, Jaeger L, Do T, Major EO, Nath A. 2015. Cell-to-cell contact  
812 facilitates HIV transmission from lymphocytes to astrocytes via CXCR4. *AIDS* 29:755.
- 813 64. Bracq L, Xie M, Benichou S, Bouchet J. 2018. Mechanisms for Cell-to-Cell  
814 Transmission of HIV-1. *Front Immunol* 9:260.
- 815 65. Geis FK, Goff SP. 2019. Unintegrated HIV-1 DNAs are loaded with core and linker  
816 histones and transcriptionally silenced. *Proc Natl Acad Sci U S A* 116:23735–23742.
- 817 66. Gélinas J-F, Gill DR, Hyde SC. 2018. Multiple Inhibitory Factors Act in the Late Phase  
818 of HIV-1 Replication: a Systematic Review of the Literature. *Microbiol Mol Biol Rev*

- 819 82:e00051-17.
- 820 67. Anderson DJ, Le Grand R. 2014. Cell-associated HIV mucosal transmission: the  
821 neglected pathway. *J Infect Dis* 210 Suppl:S606-8.
- 822 68. Quayle AJ, Xu C, Mayer KH, Anderson DJ. 1997. T Lymphocytes and Macrophages,  
823 but Not Motile Spermatozoa, Are a Significant Source of Human Immunodeficiency  
824 Virus in Semen. *J Infect Dis* 176:960–968.
- 825 69. Sadri-Ardekani H, Mizrak SC, Van Daalen SKM, Korver CM, Roepers-Gajadien HL,  
826 Koruji M, Hovingh S, De Reijke TM, De La Rosette JJMCH, Van Der Veen F, De  
827 Rooij DG, Repping S, Van Pelt AMM. 2009. Propagation of human spermatogonial  
828 stem cells in vitro. *JAMA - J Am Med Assoc* 302:2127–2134.
- 829 70. Mizuno Y, Gotoh A, Kamidono S, Kitazawa S. 1993. [Establishment and  
830 characterization of a new human testicular germ cell tumor cell line (TCam-2)]. *Nihon*  
831 *Hinyokika Gakkai Zasshi* 84:1211–8.
- 832 71. Goujon C, Malim MH. 2010. Characterization of the alpha interferon-induced  
833 postentry block to HIV-1 infection in primary human macrophages and T cells. *J Virol*  
834 84:9254–66.
- 835 72. Camus C, Matusali G, Bourry O, Mahe D, Aubry F, Bujan L, Pasquier C, Massip P,  
836 Ravel C, Zirafi O, Munch J, Roan NR, Pineau C, Dejuq-Rainsford N. 2016.  
837 Comparison of the effect of semen from HIV-infected and uninfected men on CD4+ T-  
838 cell infection. *AIDS* 30:1197–208.
- 839 73. Deleage C, Moreau M, Rioux-Leclercq N, Ruffault A, Jégou B, Dejuq-Rainsford N,  
840 Jegou B, Dejuq-Rainsford N. 2011. Human Immunodeficiency Virus Infects Human  
841 Seminal Vesicles in Vitro and in Vivo. *Am J Pathol* 179:2397–2408.
- 842 74. Jochems SP, Petitjean G, Kunkel D, Liovat A-S, Ploquin MJ, Barré-Sinoussi F, Lebon  
843 P, Jacquelin B, Müller-Trutwin MC. 2015. Modulation of type I interferon-associated  
844 viral sensing during acute simian immunodeficiency virus infection in African green  
845 monkeys. *J Virol* 89:751–62.
- 846 75. Deleage C, Wietgreffe SW, Del Prete G, Morcock DR, Hao XP, Piatak M, Bess J,  
847 Anderson JL, Perkey KE, Reilly C, McCune JM, Haase AT, Lifson JD, Schacker TW,  
848 Estes JD, Prete G Del, Morcock DR, Hao XP, Piatak M, Jr., Bess J, Anderson JL,  
849 Perkey KE, Reilly C, McCune JM, Haase AT, Lifson JD, Schacker TW, Estes JD.  
850 2016. Defining HIV and SIV Reservoirs in Lymphoid Tissues. *Pathog Immun* 1:68.
- 851 76. Demaison C, Parsley K, Brouns G, Scherr M, Battmer K, Kinnon C, Grez M, Thrasher  
852 AJ. 2002. High-Level Transduction and Gene Expression in Hematopoietic  
853 Repopulating Cells Using a Human Immunodeficiency Virus Type 1-Based Lentiviral  
854 Vector Containing an Internal Spleen Focus Forming Virus Promoter. *Hum Gene Ther*  
855 13:803–813.
- 856 77. Naldini L, Blomer U, Gallay P, Ory D, Mulligan R, Gage FH, Verma IM, Trono D.  
857 1996. In Vivo Gene Delivery and Stable Transduction of Nondividing Cells by a  
858 Lentiviral Vector. *Science (80- )* 272:263–267.
- 859 78. Helseth E, Kowalski M, Gabuzda D, Olshevsky U, Haseltine W, Sodroski J. 1990.  
860 Rapid complementation assays measuring replicative potential of human  
861 immunodeficiency virus type 1 envelope glycoprotein mutants. *J Virol* 64:2416–20.
- 862 79. Holl V, Xu K, Peressin M, Lederle A, Biedma ME, Delaporte M, Decoville T, Schmidt  
863 S, Laumond G, Aubertin AM, Moog C. 2010. Stimulation of HIV-1 Replication in  
864 Immature Dendritic Cells in Contact with Primary CD4 T or B Lymphocytes. *J Virol*  
865 84:4172–4182.
- 866 80. Adachi A, Gendelman HE, Koenig S, Folks T, Willey R, Rabson A, Martin MA. 1986.  
867 Production of acquired immunodeficiency syndrome-associated retrovirus in human  
868 and nonhuman cells transfected with an infectious molecular clone. *J Virol* 59:284–91.

- 869 81. Freed EO, Englund G, Martin MA. 1995. Role of the basic domain of human  
870 immunodeficiency virus type 1 matrix in macrophage infection. *J Virol* 69:3949–54.
- 871 82. Papkalla A, Münch J, Otto C, Kirchhoff F. 2002. Nef enhances human  
872 immunodeficiency virus type 1 infectivity and replication independently of viral  
873 coreceptor tropism. *J Virol* 76:8455–9.
- 874 83. Matusali G, Potestà M, Santoni A, Cerboni C, Doria M. 2012. The Human  
875 Immunodeficiency Virus Type 1 Nef and Vpu Proteins Downregulate the Natural  
876 Killer Cell-Activating Ligand PVR. *J Virol* 86:4496–4504.
- 877 84. Vandergeeten C, Fromentin R, Merlini E, Lawani MB, DaFonseca S, Bakeman W,  
878 McNulty A, Ramgopal M, Michael N, Kim JH, Ananworanich J, Chomont N. 2014.  
879 Cross-clade ultrasensitive PCR-based assays to measure HIV persistence in large-  
880 cohort studies. *J Virol* 88:12385–96.
- 881 85. Wang M, Liu X, Chang G, Chen Y, An G, Yan L, Gao S, Xu Y, Cui Y, Dong J, Chen  
882 Y, Fan X, Hu Y, Song K, Zhu X, Gao Y, Yao Z, Bian S, Hou Y, Lu J, Wang R, Fan Y,  
883 Lian Y, Tang W, Wang Y, Liu J, Zhao L, Wang L, Liu Z, Yuan R, Shi Y, Hu B, Ren  
884 X, Tang F, Zhao X-Y, Qiao J. 2018. Single-Cell RNA Sequencing Analysis Reveals  
885 Sequential Cell Fate Transition during Human Spermatogenesis. *Cell Stem Cell*  
886 23:599-614.e4.
- 887 86. Darde TA, Sallou O, Becker E, Evrard B, Monjeaud C, Le Bras Y, Jégou B, Collin O,  
888 Rolland AD, Chalmel F. 2015. The ReproGenomics Viewer: An integrative cross-  
889 species toolbox for the reproductive science community. *Nucleic Acids Res* 43:W109–  
890 W116.
- 891 87. Darde TA, Lecluze E, Lardenois A, Stévant I, Alary N, Tüttelmann F, Collin O, Nef S,  
892 Jégou B, Rolland AD, Chalmel F. 2019. The ReproGenomics Viewer: A multi-omics  
893 and cross-species resource compatible with single-cell studies for the reproductive  
894 science community. *Bioinformatics* 35:3133–3139.
- 895 88. Chalmel F, Primig M. 2008. The Annotation, Mapping, Expression and Network  
896 (AMEN) suite of tools for molecular systems biology. *BMC Bioinformatics* 9:86.
- 897 89. Hermann BP, Cheng K, Singh A, Roa-De La Cruz L, Mutoji KN, Chen IC,  
898 Gildersleeve H, Lehle JD, Mayo M, Westernströer B, Law NC, Oatley MJ, Velte EK,  
899 Niedenberger BA, Fritze D, Silber S, Geyer CB, Oatley JM, McCarrey JR. 2018. The  
900 Mammalian Spermatogenesis Single-Cell Transcriptome, from Spermatogonial Stem  
901 Cells to Spermatids. *Cell Rep* 25:1650-1667.e8.
- 902 90. Benjamini Y, Hochberg Y. 1995. Controlling the False Discovery Rate: A Practical and  
903 Powerful Approach to Multiple Testing. *J R Stat Soc Ser B* 57:289–300.

904

905

906

907 **Figure legends**

908 **Fig. 1 Characterisation and purity of primary TGCs**

909 (A, B) DRAQ5 DNA intercalating agent detection in flow cytometry on isolated TGCs  
910 showed the presence of haploid (n DNA, green), diploid (2n DNA, pink) and tetraploid cells  
911 (4n DNA, blue) (representative profile in A). (C, E) As expected, DDX4 labelled most germ  
912 cells irrespective of their ploidy, whereas MAGEA4 labelled early diploid and tetraploid germ  
913 cells (representative profile in C). (D, E) Somatic cell contaminants analysis in isolated TGC  
914 populations labeled with DRAQ-5 using flow cytometry and antibodies specific for somatic  
915 cells (class I HLA and vimentin) and leukocyte antigen CD45 (representative profile in D).

916

917 **Fig. 2 HIV-1 binding to primary TGCs**

918 TGCs isolated from 9 donors or PBMCs used as a positive control were tested for their ability  
919 to capture: (A) lab-adapted HIV-1 R5<sub>SF162</sub>, HIV-1 X4<sub>IIIb</sub> or (B) primary R5 and R5X4 strains  
920 following a 2h incubation at 37°C with the indicated amount of virus, as measured by p24  
921 ELISA on cell lysates following thorough washes and deduction of p24 background measured  
922 in wells with no cells. Pronase treatment post-binding was used as a negative control to ensure  
923 measure specificity. Each donor is represented by a specific symbol. (C) Pronase treatment of  
924 TGCs prior HIV R5<sub>SF162</sub> exposure (25ng p24) abrogated viral binding (n=5). Statistical  
925 analysis with non-parametric test: Wilcoxon test. \* p< 0.05.

926

927 **Fig. 3 HIV-1 alternative receptors expression by primary TGCs and HIV-1 binding**

928 **inhibition**

929 (A) Representative profiles of membrane expression of HIV receptors on the whole  
930 population of TGC (red) and the n (green), 2n (pink) and 4n DNA (blue) TGC populations.  
931 Immunolabeling was performed using specific antibodies against CD4, CCR5, CXCR4,

932 CCR3, GalCer or HSPGs, or, in the case of CD206, after detection of biotinylated-BSA-  
933 Mannose (BMA) ligand in the presence (dot-lined histogram) or absence (filled histogram) of  
934 mannan competitor. BSA was used as control (open histogram). Cells were further stained  
935 with DRAQ-5 for ploidy profile. Specific antibody detection was ensured using isotypes as  
936 controls, except for HSPGs where pronase treatment was used. Left panel shows positive  
937 controls for each receptor. **(B)** The table shows for each receptor the percentage of positive  
938 patients, the median and range of positive cells percentage. **(C)** HIV binding was measured  
939 after incubation of TGCs with HIV R5<sub>SF162</sub> (25ng p24) in the presence or absence of CD206  
940 BSA-mannose competitor (BMA), Galactosylceramide specific Mab, HSPGs competitor  
941 (heparin) at the 3 indicated doses. Results represent the mean +/- SEM of 3 to 6 independent  
942 experiments performed in duplicate and are expressed relative to their respective controls  
943 (virus-cell incubation without receptor inhibitors, or in presence of BSA for BSA-mannose).  
944 **(D)** TGCs obtained from 4 donors were incubated for 2h at 37°C with *env* deleted or HIV-1  
945 *env* expressing pseudoviruses (25 ng p24) and p24 antigen measured by ELISA. **(E)** Viral *env*  
946 neutralization was performed in the presence of gp-120 specific antibody (n=3). In all  
947 experiments, background p24 levels measured in wells without cells was deduced from the  
948 values obtained with cells. Statistical analysis with non parametric test : Wilcoxon \*: p<0.05.

949

#### 950 **Fig. 4 HIV entry in primary TGC following cell-associated infection**

951 **(A)** TGC pre-labelled with CellTracker (blue) were exposed for 18h to cell free wild type R5  
952 HIV-1 or mock exposed. Cells were co-stained for p24 (red) and DDX4 (green) and p24  
953 localization assessed by confocal microscopy Mock shows absence of labelling with DDX4  
954 antibody isotype (IgG). **(B)** TGC pre-labelled with CellTracker (blue) were exposed for 18h  
955 to R5 HIV-1<sup>GFP-Vpr</sup> viral particles (green) or mock exposed. Rare viral entry events (arrows) in  
956 cells labelled with DDX4 specific antibody (red) were visualized by confocal microscopy.

957 Mock shows absence of labelling with DDX4 antibody isotype (IgG). (C) Potential HIV  
958 receptors was assessed on the surface of Tcam-2 cells labelled for DDX4 using specific  
959 antibodies against CD4, CCR5, CXCR4, CCR3, GalactosylCeramide (GalCer) and HSPGs, or  
960 following detection of BSA-Mannose, a ligand for mannose receptor. Immunolabelling was  
961 analyzed by flow cytometry. (D) HIV-1 entry (arrows) was assessed in CFSE-labelled Tcam-  
962 2 cells (in green) exposed for 4h to a primary R5-tropic HIV-1 strain (ES X-2556-3) or mock  
963 exposed, before immunolabelling with p24 antibody (red). Nuclei were stained with DAPI  
964 (blue). (E) HIV-1 reverse transcription was assessed by qPCR on Tcam-2 cells cultured 24h  
965 with or without the reverse transcriptase inhibitor nevirapin, following exposure to HIV R5<sub>JR</sub>-  
966 CSF (n=6). (F, G) TGC pre-labelled with CellTracker (blue) were incubated for 18h with either  
967 PBMCs infected with a primary R5-tropic HIV-1 strain or mock infected (F), or with Jurkat  
968 cells infected with HIV-1 R5 or X4 strains (G). Cells were co-stained for p24 (red) and DDX4  
969 (green) or with control IgG (shown here on mock). (A, B, G) Z-stacks maximum projection  
970 are presented along with cross-sectional YZ orthogonal viewing from indicated positions (a,  
971 b) to discriminate entering viral particles (white arrow) from membrane bound viruses  
972 (arrowhead). Nuclei are stained with DRAQ5 (cyan). Scale bars = 10µm.

973

974 **Fig. 5 HIV-1 integration in testicular germ cell genome and *in vivo* detection of HIV and**  
975 **SIV DNA in human and non-human primate testicular germ cells**

976 (A-C) HIV-1 integration in primary TGCs. (A) Experimental design: after overnight contact  
977 with Jurkat cells infected with HIV-1 *nef-ires-GFP*, TGCs were recovered following CD45  
978 magnetic selection and put in culture for 5 days. The cells were then submitted to FACS  
979 sorting for live cells, negative for leukocytes markers CD45, CD3 and HLA-DR and positive  
980 for germ cell markers DDX4 and MAGEA4. As a negative control, TGCs purified by CD45  
981 magnetic selection immediately after contact with Jurkat cells were sorted by FACS similarly

982 to the overnight incubated samples. **(B)** Gating strategy and representative profile of purified  
983 live germ cells. Live single cells were selected based on absence of detection of leukocytes  
984 markers CD3, HLA-DR and CD45 and on positive expression of DDX4 and MageA4+ germ  
985 cell markers. Control antibodies are shown on bottom panel. **(C)** HIV-1 integrated DNA was  
986 measured by Alu-gag PCR on 10,000 sorted TGCs exposed to Jurkat cells for 2h without  
987 culture or after 3 to 7 days of culture following ON exposure to Jurkat cells, in 3 independent  
988 experiments. Statistical analysis with non-parametric test: Wilcoxon test. \*  $p < 0.05$ . **(D-F)**  
989 HIV integration in Tcam-2. **(D)** HIV-1 integrated DNA was measured on Tcam-2 either  
990 cultured for 48h following exposure to R5<sub>JR-CSF</sub> HIV-1 (cell-free) or exposed ON to Jurkat  
991 infected with HIV R5<sub>JR-CSF</sub>, purified by CD45 magnetic selection, cultured for 5 days and  
992 FACS sorted for CD45 negative live cells (cell associated). **(E, F)** HIV-1 reverse transcription  
993 and integration were assessed on Tcam-2 cells exposed to VSV-G- pseudotyped HIV-1. **(E)**  
994 Reverse transcripts were detected after 24h culture with or without reverse transcriptase  
995 inhibitor nevirapine (n=6) and **(F)** HIV-1 integration assessed by Alu-gag PCR in Jurkat cells  
996 (Jk) and in Tcam-2 in the presence or absence of reverse transcriptase inhibitor (n=3). **(G)** *In*  
997 *vivo* detection of HIV and SIV DNA in human and non-human primate testicular germ cells  
998 by DNAscope. Representative pictures of TGC (green) harbouring viral DNA (red) within  
999 testis tissue section from one HIV-1 infected man (VL=51 681 cp/mL), one chronically  
1000 infected rhesus macaque (VL>10<sup>6</sup> cp/mL) and one African Green monkey 64 days post  
1001 infection (VL=12085 cp/mL). Scale bars= 100µm.

1002

### 1003 **Fig. 6 HIV replication in TGCs**

1004 **(A, B)** Early HIV-1 replication in germ cells following contact with Jurkat cells infected with  
1005 HIV-1-*nef*-ires-GFP. **(A)** TGCs incubated with infected Jurkat cells were purified using  
1006 magnetic beads selection for CD45 and cultured for 9 to 12 days before co-labelling for

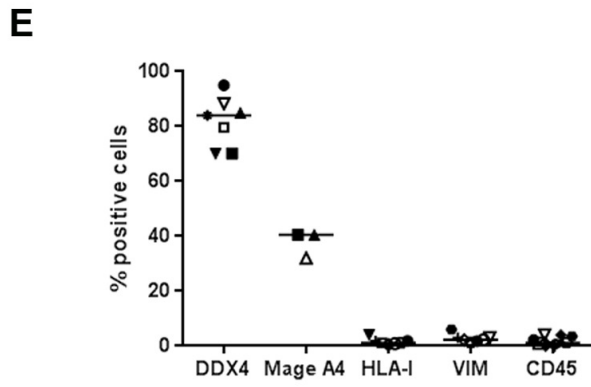
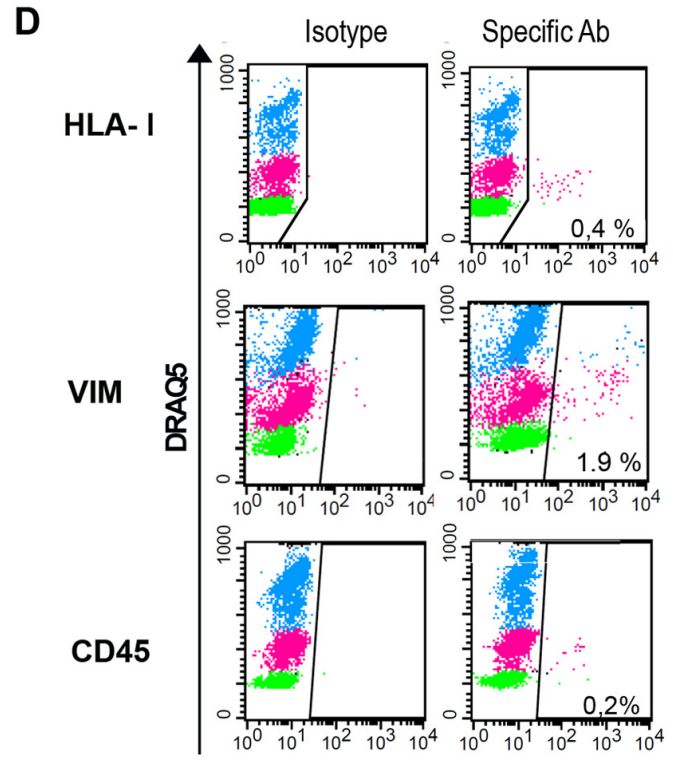
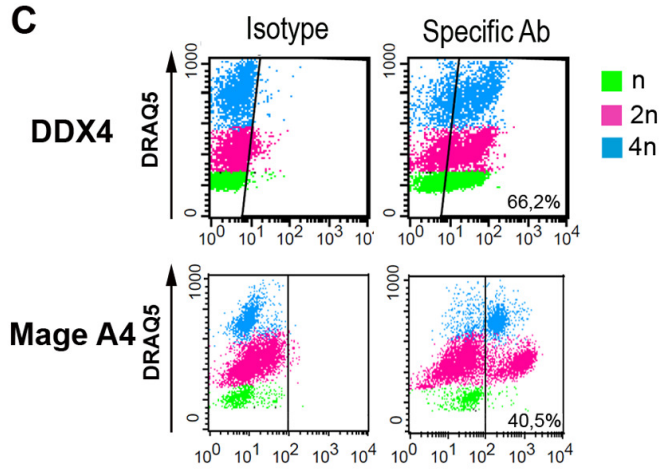
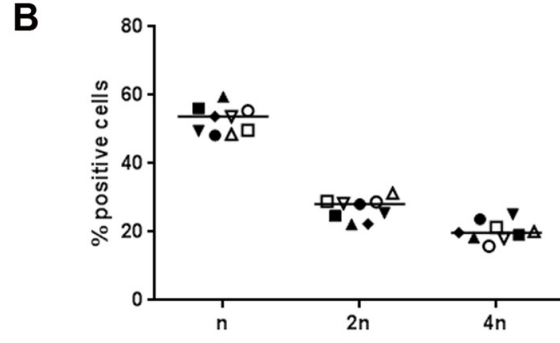
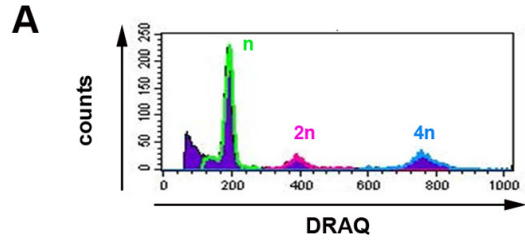
1007 DDX4 and CD45 (A, upper panel) or DDX4 and MAGE-A4 markers (A, lower panel).  
1008 Confocal images show DDX4+ germ cells and MAGEA+DDX4+ early germ cells expressing  
1009 Nef-GFP. Nuclei were stained with DAPI (blue). Scale bars = 10µm. (B) Tcam-2 cells  
1010 incubated for 18h with Jurkat infected cells and further cultured for 9 days with or without  
1011 nevirapine. Cells were stained with CD45-PE to discriminate Tcam-2 cells (CD45 negative)  
1012 from residual Jurkat cells (CD45 positive) and analyzed by flow cytometry for nef-gfp  
1013 expression. Number of gfp positive events are indicated in the plot. (C-E) HIV-1 replication  
1014 after Tcam-2 exposure to VSV-G- pseudotyped HIV-1. Viral proteins nef-GFP and p24  
1015 expression were detected by flow cytometry in Tcam-2 cells cultured for 5 days with or  
1016 without nevirapine (C). Viral production in infected T-cam2 cells cultured for 5 and 9 days  
1017 with or without RT or integrase inhibitor (raltegravir) was assessed by measuring intracellular  
1018 p24 in ELISA (D). Infectious viral particles release was assessed by exposing PBMCs for 4h  
1019 to T-cam2 cell supernatants collected at day 5 and 9 post-infection. p24 was measured by  
1020 ELISA in supernatants from exposed PBMC at the indicated time points (E). Data shown are  
1021 representative of 3 independent experiments.

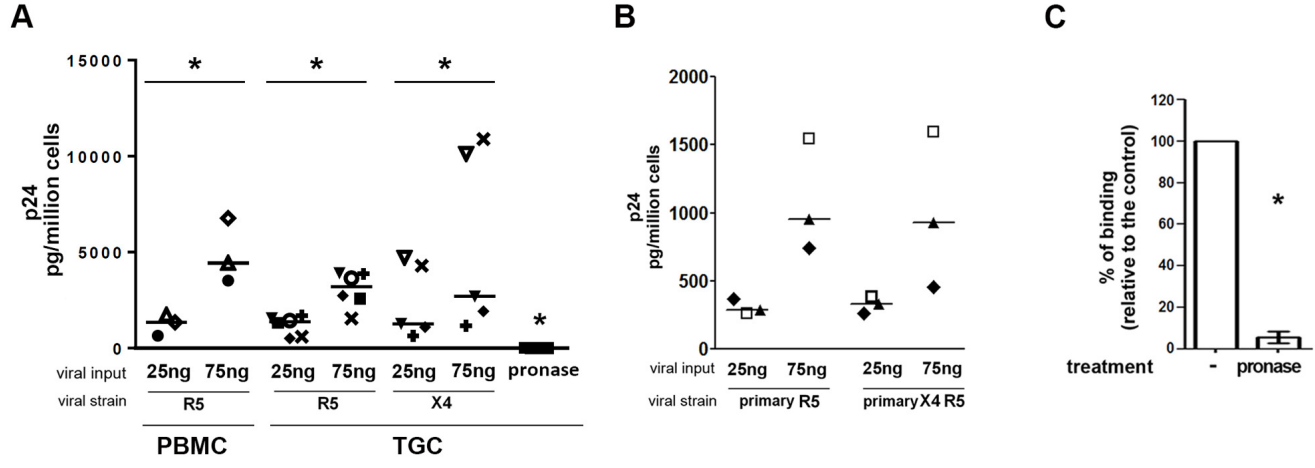
1022

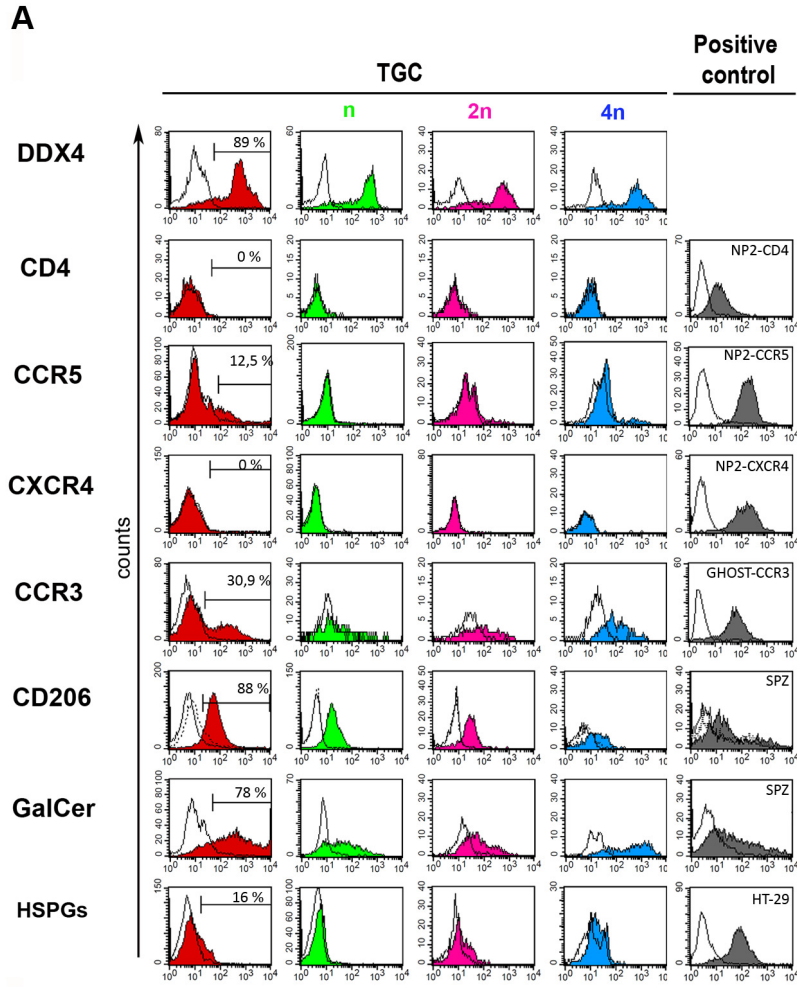
1023 **Fig. 7 Enrichment analysis of factors involved in HIV life cycle in the human testis.**

1024 Previously published single-cell RNA-sequencing data of human adult testis (85) were used to  
1025 identify differentially-expressed (DE) genes showing peak expression in testicular  
1026 macrophages (TM, 729 genes), Sertoli cells (SC, 1,926 genes), spermatogonia (SPG, 2,718  
1027 genes), spermatocytes (SPC, 4,781 genes) or spermatids (SPT, 2,502 genes), including 283  
1028 factors involved in HIV life cycle (out of an initial set of 335 factors retrieved from the  
1029 literature). The over- or under-representation of these factors considered according to  
1030 different categories (“Early Co-factors”, “Late Co-factors”, “Sensors”, “Early Inhibitors” and  
1031 “Late Inhibitors”) was then evaluated in each expression cluster by means of a

1032 hypergeometric test. Rectangles indicate the observed (left) and expected (right) numbers of  
1033 genes for each type of factors in each expression cluster, as well as the corresponding p-  
1034 values adjusted by the Benjamini-Hochberg procedure. Enrichments and depletions are  
1035 indicated in red and blue, respectively, according to the scale bar.

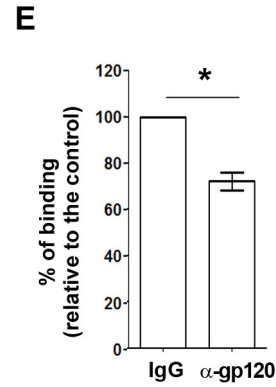
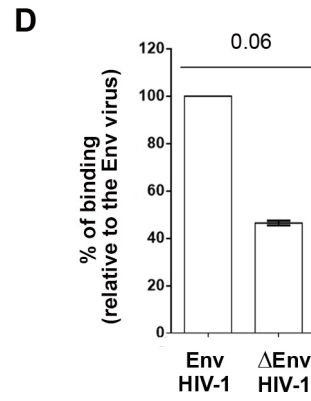
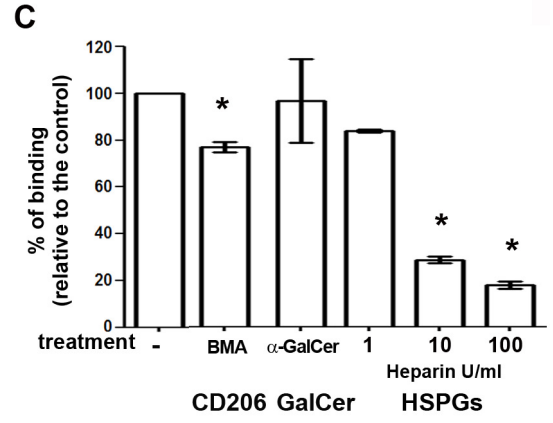


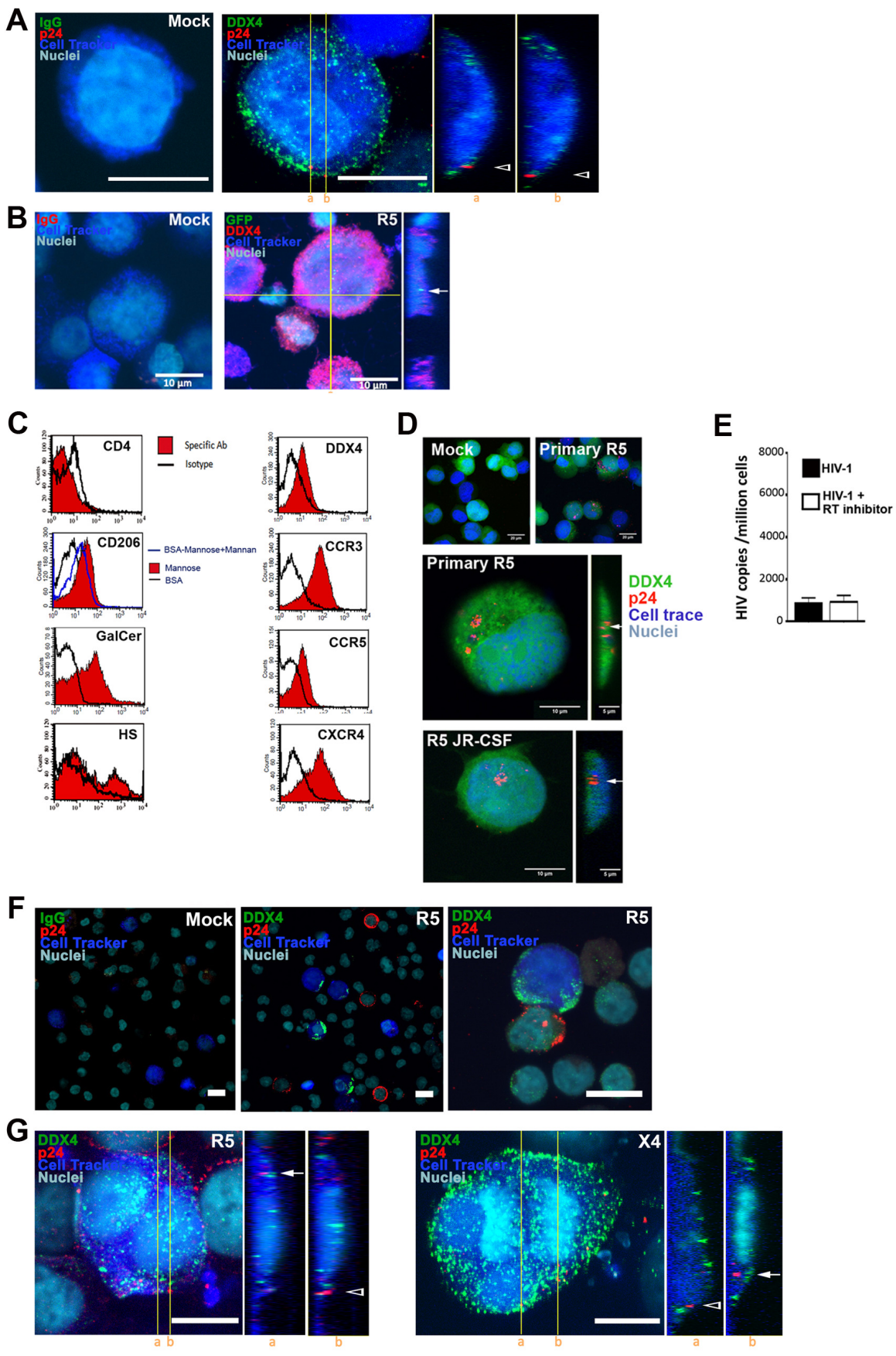


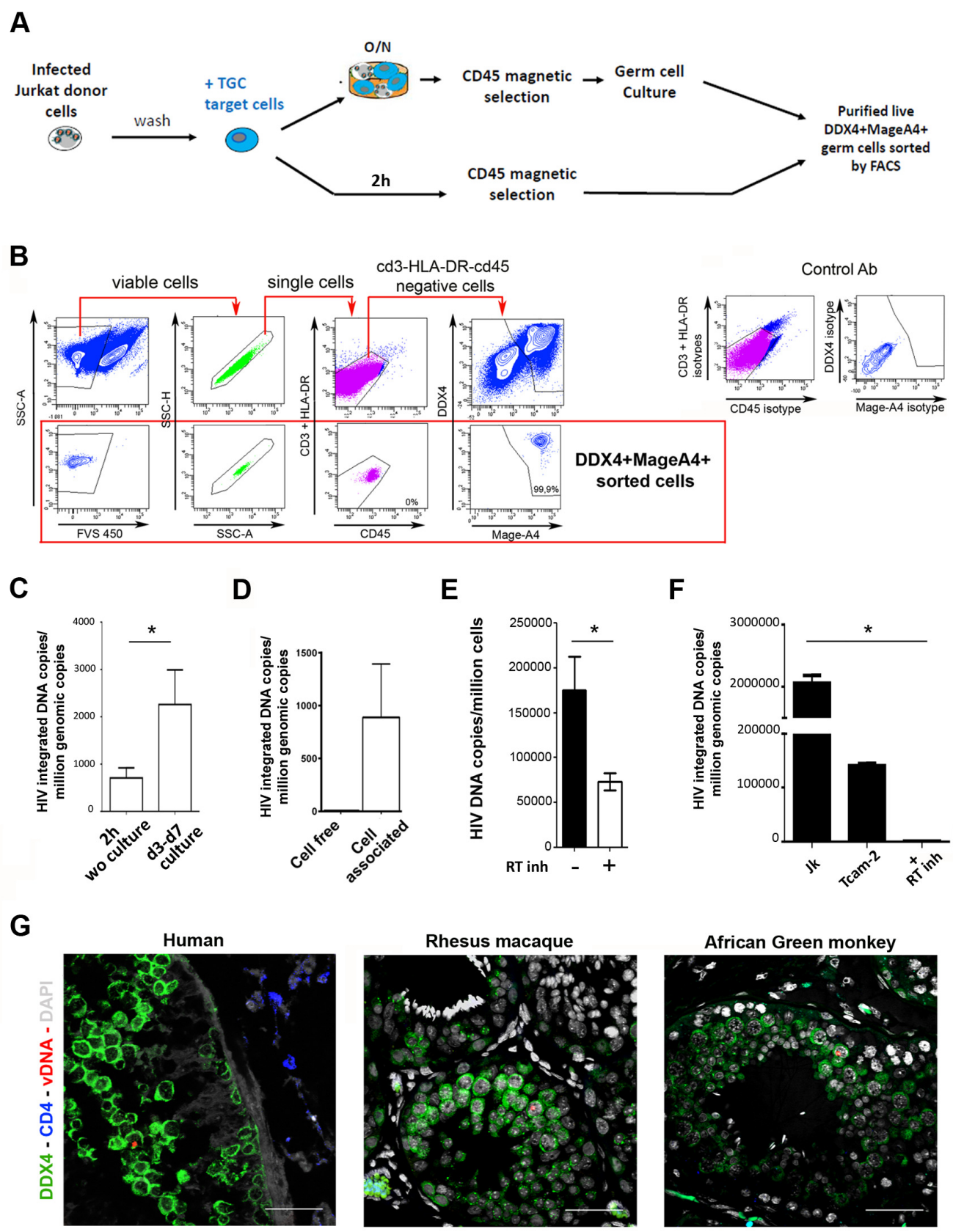


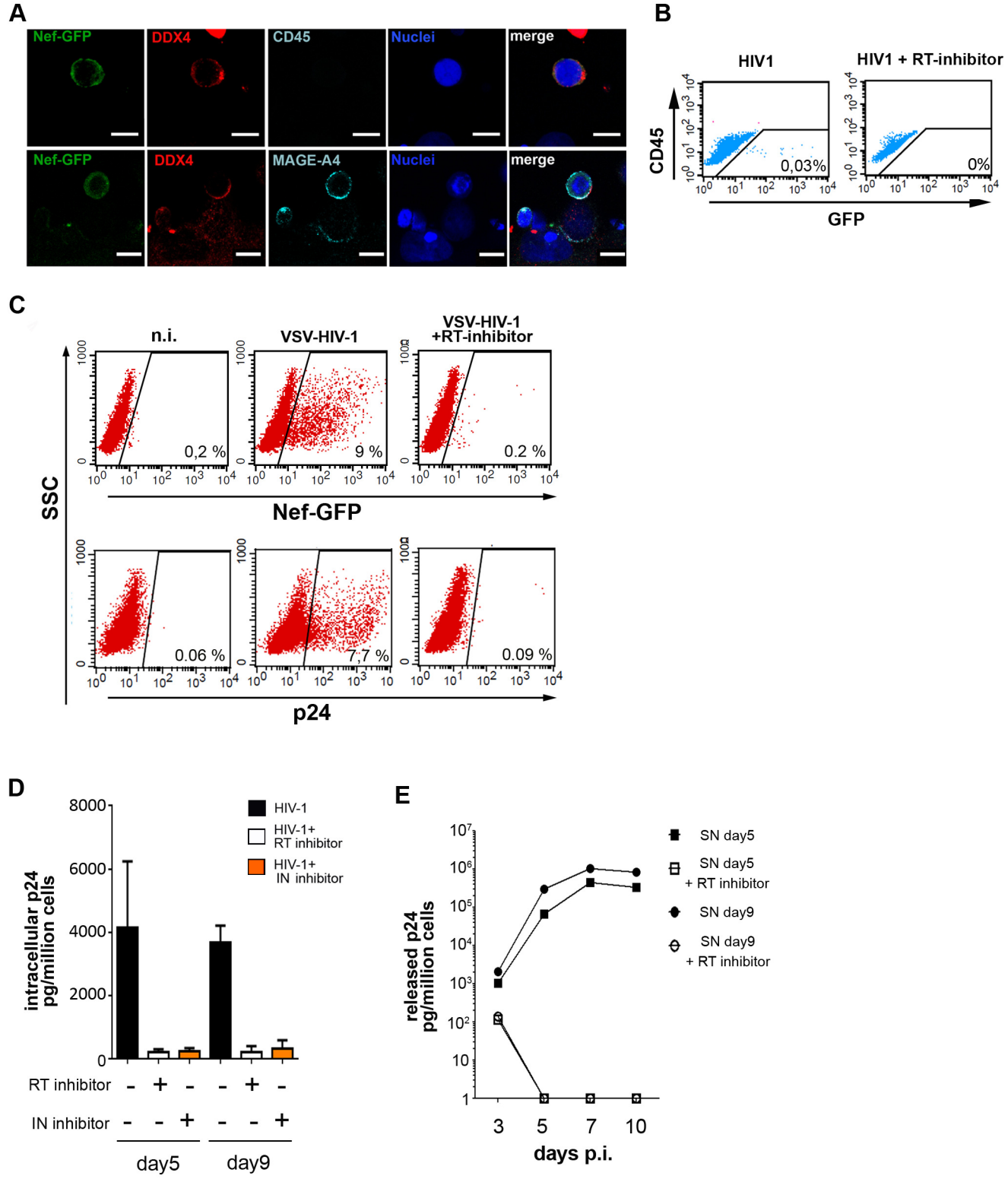
**B**

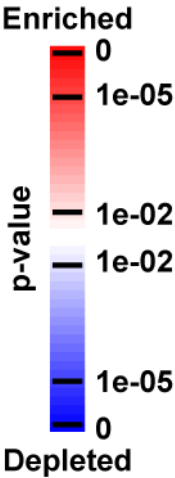
	% positive patients n=8-10	% positive cells median (min-max)
CD4	0	
CCR5	50	4.6 (2.5-12.5)
CXCR4	0	
CCR3	100	25.9 (14.2-45)
CD206	100	74.3 (51.5-90.5)
GalCer	100	77.5 (51.2-91.2)
HSPGs	100	7.1 (2.7-16)









		TM	SC	SPG	SPC	SPT	
<b>DE Genes</b>	12656	729	1926	2718	4781	2502	
<b>Sensors</b>	13	<b>7 / 1</b> <b>7.76e-6</b>	3 / 2 5.00e-1	2 / 3 5.00e-1	<b>0 / 5</b> <b>6.26e-3</b>	1 / 3 4.79e-1	<b>Enriched</b>  <b>p-value</b> <b>Depleted</b>
<b>Early Inhibitors</b>	22	<b>5 / 1</b> <b>1.45e-2</b>	8 / 3 7.40e-2	3 / 5 5.00e-1	<b>3 / 8</b> <b>2.59e-2</b>	3 / 4 5.00e-1	
<b>Late Inhibitors</b>	152	<b>30 / 9</b> <b>1.33e-8</b>	32 / 23 9.76e-2	<b>46 / 33</b> <b>2.03e-2</b>	<b>34 / 57</b> <b>1.95e-4</b>	<b>10 / 30</b> <b>2.38e-5</b>	
<b>Early Co-factors</b>	71	4 / 4 5.00e-1	7 / 11 5.00e-1	<b>30 / 15</b> <b>3.80e-4</b>	22 / 27 2.16e-1	8 / 14 1.28e-1	
<b>Late Co-factors</b>	25	2 / 1 5.00e-1	4 / 4 5.00e-1	5 / 5 5.00e-1	10 / 9 5.00e-1	4 / 5 5.00e-1	